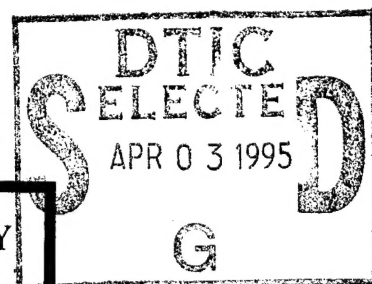


NAVAL POSTGRADUATE SCHOOL MONTEREY, CALIFORNIA



19950329 041

THESIS



**A NEW KINEMATIC MODEL FOR THE STUDY
OF THE ROLE OF THE
POSTERIOR CRUCIATE LIGAMENT (PCL)
IN HUMAN KNEE MOTION**

by

Robin L. Belen

December, 1994

Thesis Advisor:

Young W. Kwon

Approved for public release; distribution is unlimited.

REPORT DOCUMENTATION PAGE			Form Approved OMB No. 0704-0188	
Public reporting burden for this collection of information is estimated to average 1 hour per response, including the time for reviewing instruction, searching existing data sources, gathering and maintaining the data needed, and completing and reviewing the collection of information. Send comments regarding this burden estimate or any other aspect of this collection of information, including suggestions for reducing this burden, to Washington Headquarters Services, Directorate for Information Operations and Reports, 1215 Jefferson Davis Highway, Suite 1204, Arlington, VA 22202-4302, and to the Office of Management and Budget, Paperwork Reduction Project (0704-0188) Washington DC 20503.				
1. AGENCY USE ONLY (Leave blank)		2. REPORT DATE December 1994.		3. REPORT TYPE AND DATES COVERED Master's Thesis
4. TITLE AND SUBTITLE A NEW KINEMATIC MODEL FOR THE STUDY OF THE ROLE OF THE POSTERIOR CRUCIATE LIGAMENT (PCL) IN HUMAN KNEE MOTION			5. FUNDING NUMBERS	
6. AUTHOR(S) ROBIN LYNN BELEN				
7. PERFORMING ORGANIZATION NAME(S) AND ADDRESS(ES) Naval Postgraduate School Monterey CA 93943-5000			8. PERFORMING ORGANIZATION REPORT NUMBER	
9. SPONSORING/MONITORING AGENCY NAME(S) AND ADDRESS(ES)			10. SPONSORING/MONITORING AGENCY REPORT NUMBER	
11. SUPPLEMENTARY NOTES The views expressed in this thesis are those of the author and do not reflect the official policy or position of the Department of Defense or the U.S. Government.				
12a. DISTRIBUTION/AVAILABILITY STATEMENT Approved for public release; distribution is unlimited.			12b. DISTRIBUTION CODE	
13. ABSTRACT (maximum 200 words) A six degree of freedom model was utilized to study the motion of the loaded human knee joint, with emphasis placed on the role of the posterior cruciate ligament (PCL) in that motion. Unlike previous studies, where the joint was loaded statically, continuous measurements were taken throughout the range of motion, full extension (zero degrees) to 110 degrees flexion. Several different loading conditions were studied, with loading conditions varying to simulate the natural body forces (i.e. the normal condition) and hamstrings-deficient or quadriceps-deficient conditions. The motion of the knee in the normal configuration was then compared to the motions after the PCL was surgically severed. Finally, the PCL was reconstructed, the tests were repeated, and the results were compared to the normal configuration. The joint reaction forces on the knee were calculated using the normal knee configuration as the loaded condition. These comparisons will aid in determining the best method of PCL reconstruction.				
14. SUBJECT TERMS BIOMECHANICS, KNEE KINEMATICS, POSTERIOR CRUCIATE LIGAMENT			15. NUMBER OF PAGES 78	
			16. PRICE CODE	
17. SECURITY CLASSIFICATION OF REPORT Unclassified	18. SECURITY CLASSIFICATION OF THIS PAGE Unclassified	19. SECURITY CLASSIFICATION OF ABSTRACT Unclassified	20. LIMITATION OF ABSTRACT UL	

NSN 7540-01-280-5500

Standard Form 298 (Rev. 2-89)

Prescribed by ANSI Std. Z39-18 298-102

Approved for public release; distribution is unlimited.

**A NEW KINEMATIC MODEL FOR THE STUDY
OF THE ROLE OF THE POSTERIOR CRUCIATE LIGAMENT (PCL) IN HUMAN
KNEE MOTION**

by

Robin L. Belen
Lieutenant Commander, United States Navy
B.S., Pennsylvania State University, 1983

Submitted in partial fulfillment
of the requirements for the degree of

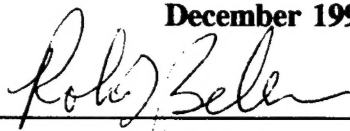
MASTER OF SCIENCE IN MECHANICAL ENGINEERING

from the

NAVAL POSTGRADUATE SCHOOL

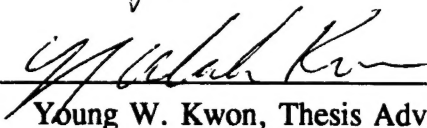
December 1994

Author:

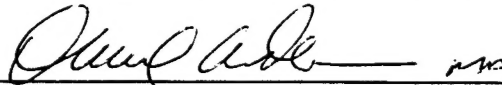


Robin L. Belen

Approved by:



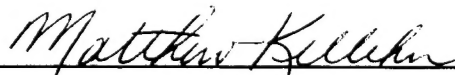
Young W. Kwon, Thesis Advisor



David P. Adkison, Second Reader



Marlene DeMaio, Second Reader



Matthew D. Kelleher, Chairman
Department of Mechanical Engineering

ABSTRACT

A six degree of freedom model was utilized to study the motion of the loaded human knee joint, with emphasis placed on the role of the posterior cruciate ligament (PCL) in that motion. Unlike previous studies, where the joint was loaded statically, continuous measurements were taken throughout the range of motion, full extension (zero degrees) to 110 degrees flexion. Several different loading conditions were studied, with loading conditions varying to simulate the natural body forces (i.e. the normal condition) and hamstrings-deficient or quadriceps-deficient conditions. The motion of the knee in the normal configuration was then compared to the motions after the PCL was surgically severed. Finally, the PCL was reconstructed, the tests were repeated, and the results were compared to the normal configuration. The joint reaction forces on the knee were calculated using the normal knee configuration as the loaded condition. These comparisons will aid in determining the best method of PCL reconstruction.

Accession For	
NTIS CRA&I	<input checked="checked" type="checkbox"/>
DTIC TAB	<input type="checkbox"/>
Unannounced	<input type="checkbox"/>
Justification	
By	
Distribution /	
Availability Codes	
Dist	Avail and/or Special
A-1	

TABLE OF CONTENTS

I. INTRODUCTION	1
II. BACKGROUND	3
III. SPECIMEN PREPARATION	13
IV. TEST EQUIPMENT	15
V. ANALYSIS	27
A. DATA INTERPRETATION	27
B. TRANSLATION COMPARISONS	29
C. ROTATION COMPARISONS	31
D. JOINT REACTION FORCES	32
VI. CONCLUSIONS	61
VII. RECOMMENDATIONS	63
GLOSSARY OF TERMS	65
LIST OF REFERENCES	67
INITIAL DISTRIBUTION LIST	71

ACKNOWLEDGEMENTS

I would like to give thanks to the Lord, our Father, for giving me the strength and courage to complete study in this field. I also count among my blessings my many friends here at the Naval Postgraduate School whose help and advice were invaluable. I am grateful to my advisor, Professor Kwon, for his patience and understanding, and to Drs. Adkison and DeMaio, for their willingness to allow me to help on this project. I thank the lab technician, Mr. Jim Scholfield, whose energy, technical expertise, and dedication were unmatched. I give special thanks to my husband, without whom none of this would have been possible.

I. INTRODUCTION

Knee injuries are surprisingly common, both in the military and in the civilian community. The requirements of military life, including physical training, running in combat boots with fully loaded packs, drilling and shipboard duties only serve to compound such injuries.

Much research has been directed to the study of anterior cruciate ligament (ACL) injuries, but very little has been done in the study of posterior cruciate ligament (PCL) injuries. Additionally, most previous research has been conducted on joints with a restricted range of motion, usually 0° to 90° flexion. Testing conditions have usually utilized a constrained model with the femur held fixed or in a rigid position while the tibia is moved. Loading conditions applied at several fixed angles have traditionally been used instead of continuous loading and continuous motion. Interpolations from such discontinuous data have been used to generate curves which supposedly represent knee kinematic behavior.

In conjunction with LCDR M. DeMaio and LCDR D. Adkison, medical doctors in the Department of Orthopaedic Surgery at Naval Hospital, Oakland, California, the motion of the human knee joint was studied. The scope of this paper will specifically address issues uncovered during the first several months of this long term effort, with the focus on the development of a new six degree of freedom knee model unlike any previously discussed. There is no indication from a literature search that research utilizing a true six degree of freedom, continuous motion model has ever been performed.

The range of motion of an intact normal knee will be studied and compared at different conditions to simulate quadriceps-deficient and hamstring-deficient conditions. Since much literature already exists on the effects of ACL injuries, PCL injuries will be targeted for this early portion

of this study. (The ACL will be investigated at a later date.) Continuous kinematics of the intact knee will be described with each knee acting as its own control for subsequent conditions. The PCL will then be severed arthroscopically and the range of motion will be tested under similar loading conditions as the normal knee. Then the PCL will be surgically reconstructed, and data collected under conditions identical to controls.

From this information, normal kinematics and pathokinematics relating to the role of the PCL is to be determined. Literature shows the PCL to be of primary importance in stabilization of the knee joint. Once the relative motion of the knee has been recorded, isolated and coupled motions for each axis and degree of freedom will be discussed. From this data, joint reaction forces will be calculated. The results will be plotted and compared across the various conditions. This will serve to direct future efforts for improvement of reconstruction techniques to adequately restore the kinematics of the PCL deficient knee to its pre-injury function.

II. BACKGROUND

Knee joint mechanics have been studied extensively. Numerous papers have been written documenting the role of the cruciate ligaments, possible replacement tissues (grafts for reconstructions), contact regions of the femur and tibia, and finite element modeling of the motion of the knee [Ref. 1-30]. A vast majority of the papers on the role of the cruciate ligaments focus on the anterior cruciate ligament (ACL) [Ref. 5, 10, 11, 15, 16]. One study specified that of a literature search conducted in 1988, 127 papers were found documenting the role of the ACL, but only 19 discussed the posterior cruciate ligament (PCL) [Ref. 19]. Epidemiologic research shows that most injuries to the PCL occur during automobile accidents or while playing sports [Ref. 12] and suggest that certain loading conditions correlated with injury to the PCL [Ref. 23]. The PCL is known to be the principal structure in preventing posterior tibial translation at all angles [Ref. 3], but especially at greater angles of flexion [Ref. 3, 7, 8]. It also deters varus and external rotation of the tibia [Ref. 3, 7, 8]. No significant differences were discovered between left and right knees [Ref. 7].

The majority of current research reviewed used fixed models (either the tibia or femur being held rigid, or in some cases, both) [Ref. 1, 2, 3, 8]. A few have discussed the use of a six degree of freedom model [Ref. 7, 9, 10, 15] but still use a static loading situation, then interpolate the results to actual knee motion. One study specified that coupled motions cannot be ignored and therefore models should not be constrained [Ref. 6]. The importance of measuring a continuous relationship between the movements of the knee ligaments and the structural bones and muscles is obvious.

Several muscle groups are responsible for controlling flexion and extension of the knee joint [Ref. 26]. The

primary flexors are the hamstrings and the gastrosoleus while the primary extensor is the quadriceps femoris (Figure 1). The ligaments function as a local controller to maintain the integrity of the joint. The surface geometry of the tibia and femur are also responsible for motion control. The surface motion patterns of the tibio-femoral joint have been described in three different patterns. These are gliding, rolling, and a glide/roll combination. Actual movement of the knee in extension occurs in three planes, discussed in detail below. An example of the importance of the three plane model is evident for a description of the 'screw home' locking mechanism (external tibial rotation as the knee is fully extended).

An anatomically based coordinate system has been proposed to serve as a reference to define the knee motion [Ref. 4, 29]. The three rotations and three translations are described as (Figure 2):

Rotation:

- a) flexion and extension in the mediolateral direction (about the x axis) (Figure 2a,2d)
- b) internal and external rotation about the axis along the tibia (about the y axis) (Figure 2b,2d)
- c) adduction and abduction occurring about the axis passing through the center of the knee in an anterior/posterior direction (about the z axis) (Figure 2c)

Translation:

- a) medial to lateral shift along the axis in the mediolateral direction (along the transepicondylar pin or x axis) (Figure 2a)
- b) compression and distraction along the superior/inferior direction of the tibia (in the y direction) (Figure 2b, 2e)
- c) anterior/posterior drawer along the axis in the

anterior/posterior direction (along the z axis)
(Figure 2c)

Each cruciate ligament has two major bands with reciprocating functions [Ref. 9]. The PCL has an anterolateral band that tenses in flexion and a posteromedial band that tenses in extension. These bands are named for their relative attachment location on both the femur (anterior or posterior) and the tibia (medial or lateral). It has been determined that depending on the flexion angle, some fibers remain taut and resist applied force, while others slacken and change direction and tighten before bearing the load. This process is called recruitment [Ref. 19]. Internal rotation has been noted to recruit cruciate ligament fibers [Ref. 21].

Ligament fibers may lengthen by up to 20% before failing in tension [Ref. 20]. The PCL may restrict motion of the tibia along the anterior/posterior drawer by tightening [Ref. 24]. It does not come into contact with the femur at any flexion angle and is influenced considerably by the quadriceps [Ref. 32]. The PCL lengthens steadily with flexion angle, but shows little change after 90 degrees flexion.

Static loading of the knee refers to rigidly fixing the tibia or femur, then flexing the other long bone until the desired angle of flexion is reached. At this flexion angle, both bones are held stationary and measurements taken on the position and condition of the ligaments. Desired forces or loading is then added and readings are taken to record the changes. Typical flexion angles of interest are 0° , 30° , 45° , 60° , and 90° [Ref. 7, 8, 22-28]. Few papers were found going beyond 90 degrees flexion [Ref. 19, 22]. It was determined [Ref. 27] that in static loading of the knee, the maximum axial force in the femur upon with knee flexion is roughly 3 1/2 to 4 1/2 times the body weight [Ref. 13], with the quadriceps tension force and the patellar reaction force roughly the same order of magnitude. Smaller forces of

constraint are present at the tibia/femur interface equal to roughly 2 1/2 to 4 times the body weight. To ensure the femoral forces act axially, the quadriceps tendon exerts a force anterior to the femoral condyles via the patella (Figure 3). With contraction of the quadriceps, the static forces transmitted at the knee joint change considerably [Ref. 27]. The bending moment in the femur is small. The main function of the patello-femoral joint is increasing the effective lever arm of the quadriceps in affecting knee extension or resisting knee flexion [Ref. 14]. It also centralizes divergent muscle groups of the quadriceps.

The presence of highly congruent load bearing joint surfaces together with menisci, ligaments, capsule and muscles (Figure 4) make the knee one of the most complex joints in the musculoskeletal system [Ref. 17, 18]. Strain is non-uniform along and across the tissue surface [Ref. 28]. The ligament strain near the bone attachment sites is higher than the mid-length region due to: variation in the fiber bundle or fascicle length within the tissue; less parallel fiber bundle alignment in ligaments; and variations in mechanical properties within the tissue.

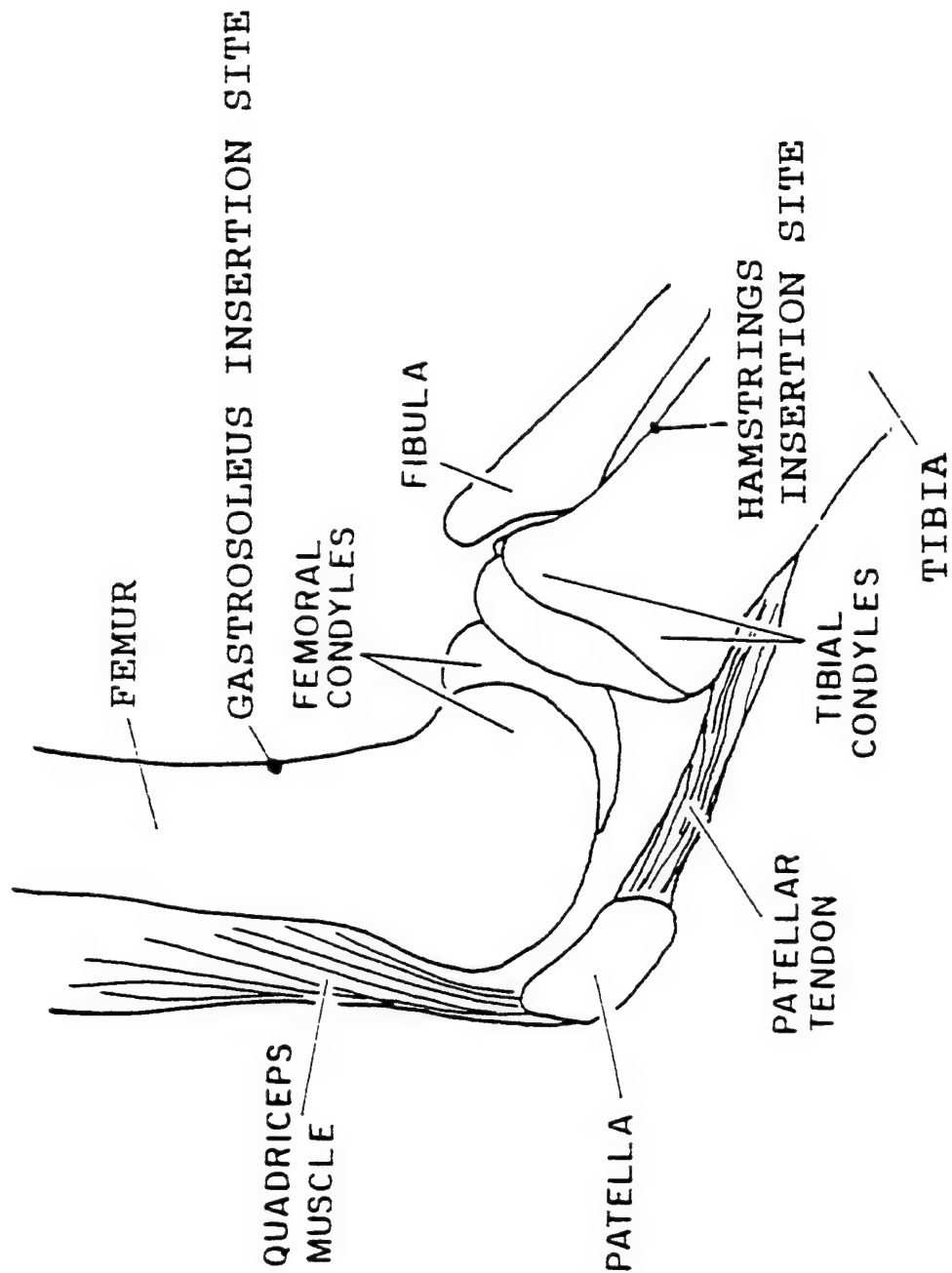


Figure 1: An overall view of the knee joint, showing the relative attachment sites of the gastrosoleus and hamstrings muscles, the quadriceps muscle, patella, and transepicondylar pin [Ref. 31].

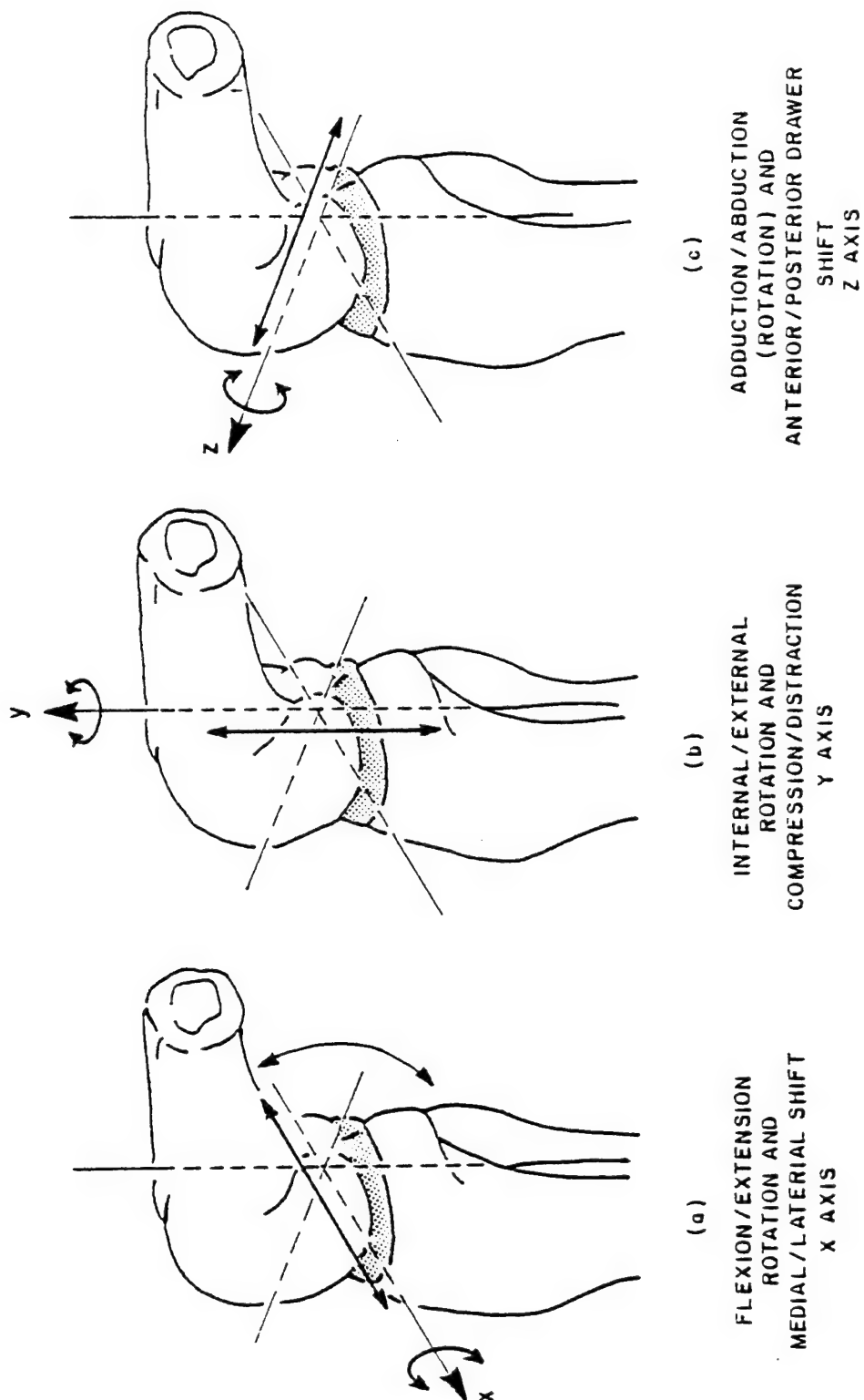


Figure 2.1: A, B, C are schematics showing the motions being studied [Ref. 31,32].

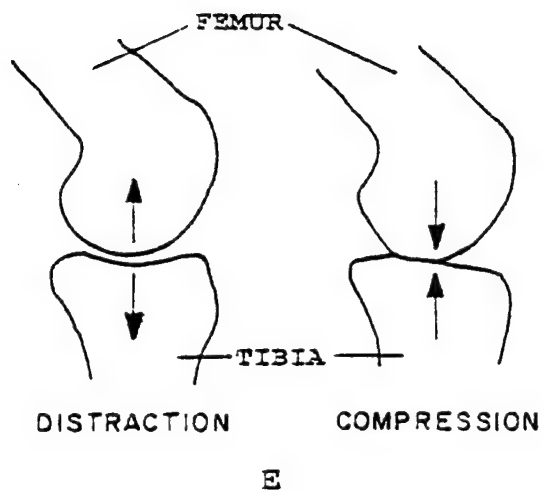
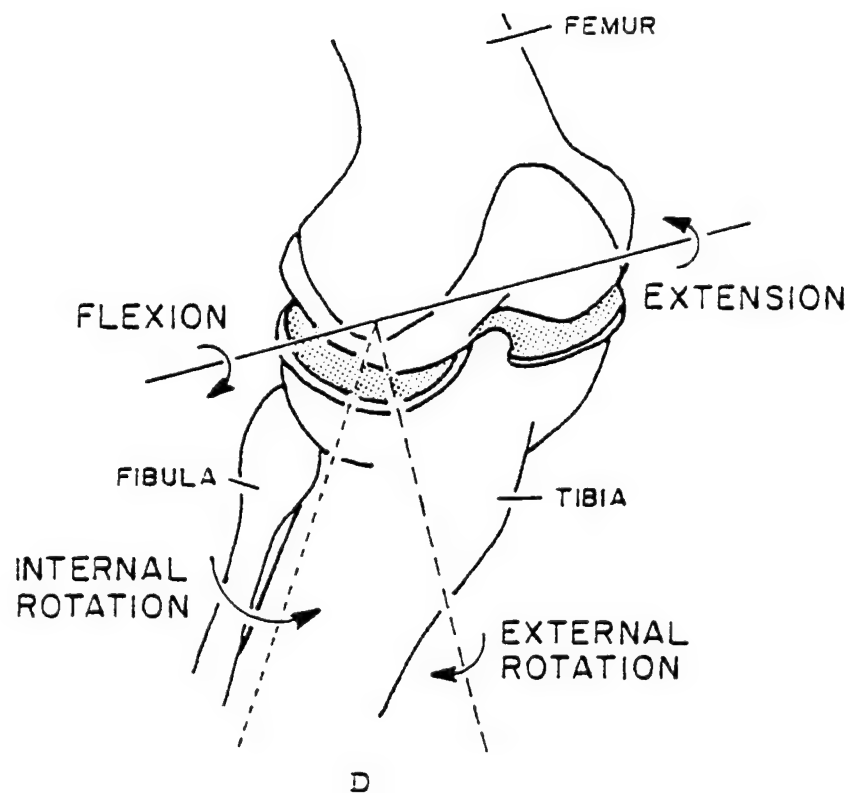


Figure 2.2: D and E provide amplification of the motions.
[Ref. 31,32].

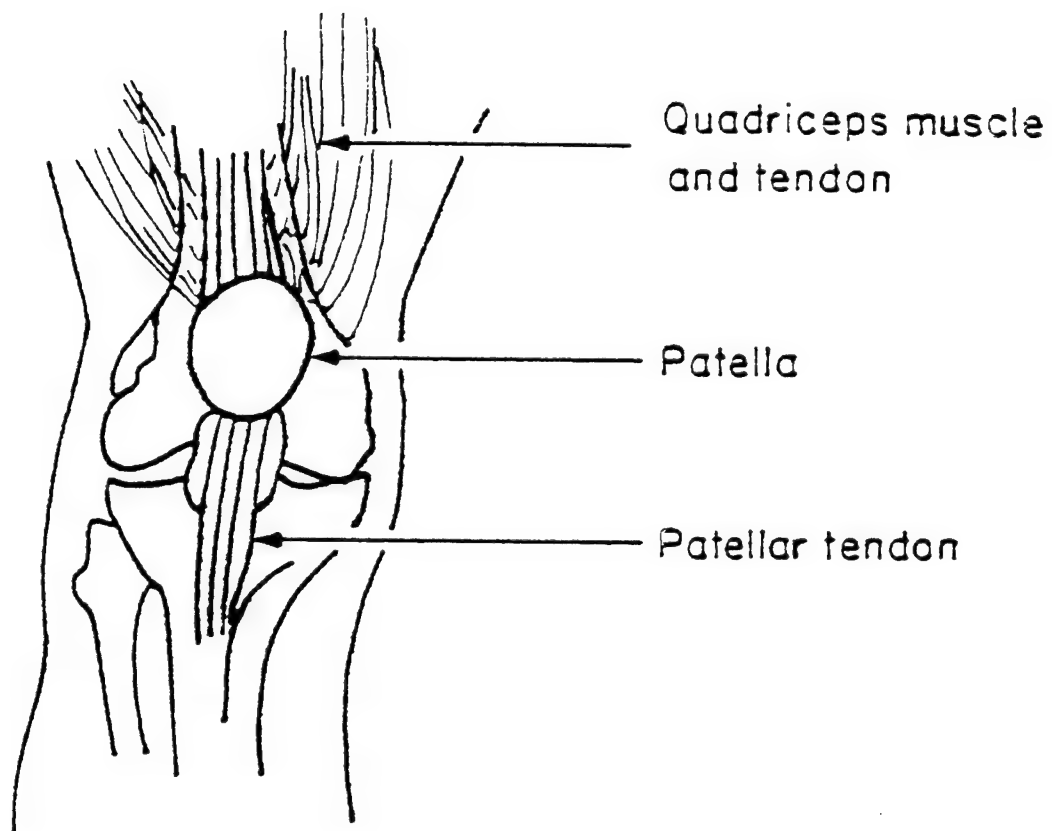


Figure 3: Schematic showing anterior view of the extensor mechanism (quadriceps muscle, patella, and patellar tendon).

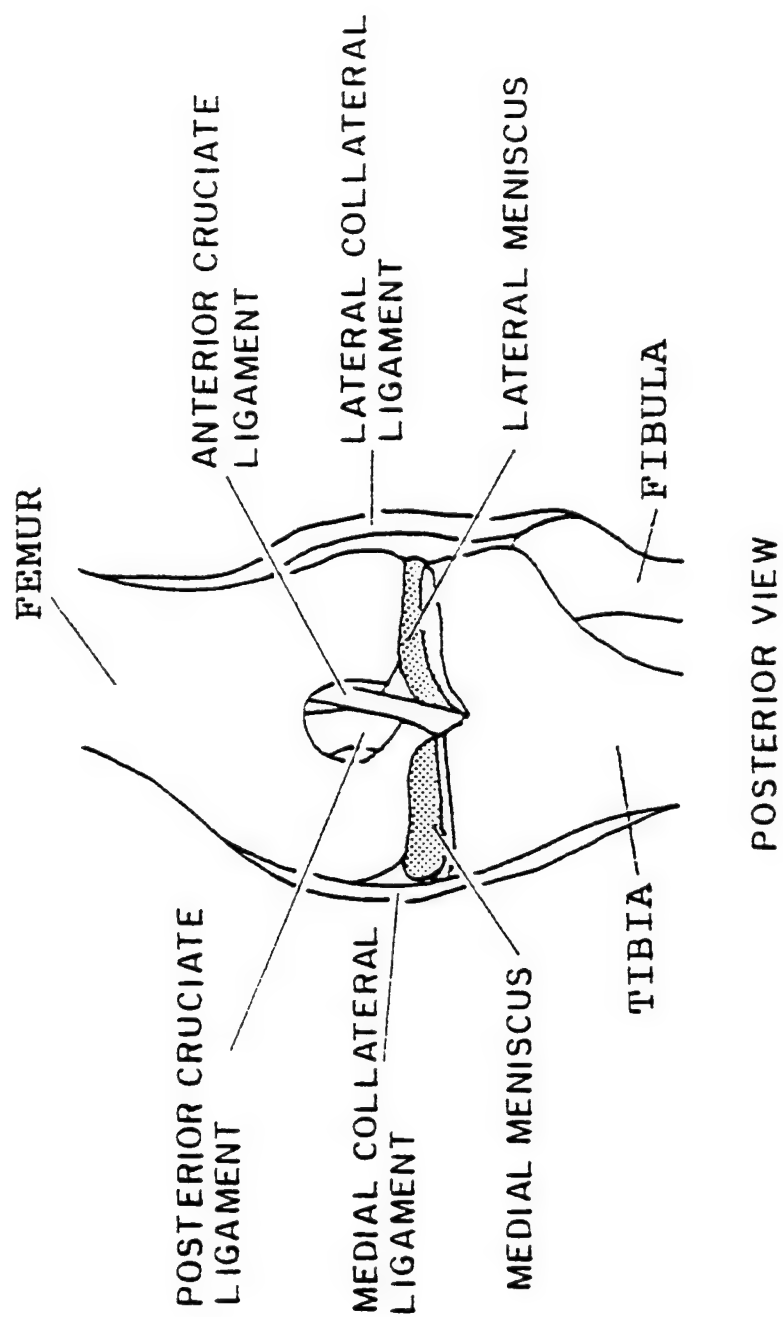


Figure 4: A detailed posterior view of knee showing insertion sites for ACL and PCL [Ref. 32].

III. SPECIMEN PREPARATION

Five right human knee joints were used in this research. The donors were four male and one female, ranging in age from 45 to 58 years old (average age 51). All donors died of natural causes with no trauma to the knee.

The knees were examined and photographed arthroscopically to confirm normal cruciate ligaments and menisci. They were then cut mid-tibia and mid-femur and kept frozen, intact, at (-15) degrees C. They were removed from the freezer the night before testing and prepared the morning of the test. Preparation included the removal of tissue leaving an intact capsule, quadriceps mechanism, and ligaments. The fibula was removed. A 10 millimeter diameter Kuntschner rod (K-rod) was cemented into the medullary canal of both the tibia and femur. The rods varied in length, depending on the size of the knee, in an effort to maintain the same distances on the test machine for consistency. Eye bolts were inserted into the bones at vector sum points for the gastrosoleus, the hamstrings and the quadriceps muscles.

A transepicondylar femoral pin was used to define a reference point and represent the center of the femoral axis of rotation. Previous studies show this is a good reference for relative motion. The instrument jig was fixed to the medial aspect of the tibia. The transducers used to measure the continuous motion of both translation and rotation were mounted to this jig. The jig underwent slight modifications upon each application in an attempt to maintain relative distances between different size knee joints (Figure 5).

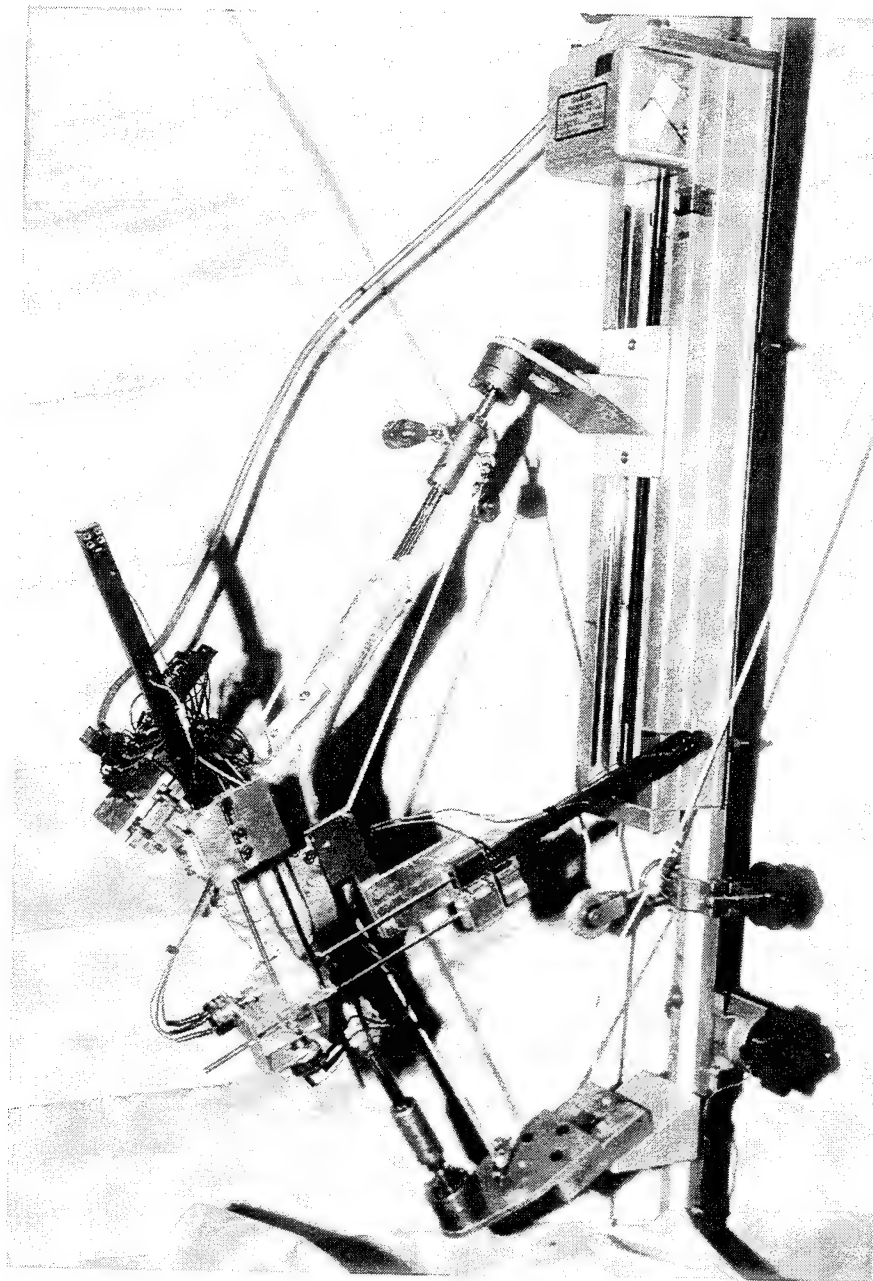


Figure 5: Photograph of actual test equipment with human knee in place. The X, Y, and Z translational potentiometers, as well as, the Y and Z rotational potentiometers are visible. Traction ropes are in place applying loads simulating live human knee.

IV. TEST EQUIPMENT

As stated, a continuous motion six degree of freedom model has yet to be reported in the literature, so a test stand had to be developed (Figures 6 and 7). In order to maintain the six degrees of freedom desired, a uniaxial ball and socket joint was chosen to be used to secure both the femur and the tibia to the test apparatus. By allowing both joints to move freely, rather than fixing one or the other as has been previously reported, a complete range of motion is maintained. The K-rods that were inserted into the medullary canals were then connected to the ball and socket joints.

With the degrees of freedom provided for, the next step was to enable and record continuous motion of flexion and extension. First, to create continuous motion, a "Velmax Unislide" worm gear drive was chosen to be attached to one end, while fixing the other. It did not matter which end was held fixed since it was to be able to rotate freely, so for ease of design of the supporting equipment, the tibia end was chosen to be held in the stationary ball and socket joint (Figure 8). The joint itself (socket) was bolted onto a plate that was then clamped to a crossbeam (1 foot x 1 in diameter staging) to which the worm gear was attached. This was supported by another crossbeam and bolted to the counter top. One large goal post type frame was made with smaller appendages rigidly attached running perpendicularly for suspension of weights (Figure 9). The other socket joint, also bolted to a plate, was bolted to the worm gear slide of the Unislide and permitted to move up and down.

The Unislide test stand set-up was carefully constructed to ensure that both ball and socket joints and the worm drive slide remained in the same plane, or collinear, to prevent induced binding. As the upper ball and socket plate traversed with the Unislide worm drive, the motion remained

parallel to the specimen. A plastic knee joint model was used to test the transverse motion to ensure accuracy prior to inserting a real human knee.

The next process allowed the weights to be added in the appropriate locations (vector sum points of the various muscle groups) to simulate loading the knee. Eye bolts were inserted below the patella at the tibial tubercle anteriorly and posteriorly at the vector sum points for the hamstrings and gastrosoleus muscles, respectively (Figure 10). Weights were attached to these eye bolts via traction rope to simulate loading. Pulleys were positioned such that the direction of the traction rope followed the path of the force being simulated. Figure 9 shows the pulleys and their usage to force the correct direction.

The next step was to devise a mechanism to record the actual motion of the knee. Because a six degree of freedom model was being developed, three translational and three rotational measurements would be needed (Figure 7). Three translational potentiometers, with a slide range of six inches were procured, as well as three rotational potentiometers. A coordinate axis system was defined such that the x axis lies along the transepicondylar pin and the y axis along the tibia (positive direction up, or towards the hip joint). Then using the right hand rule, the z axis is perpendicular to the x-y plane, coming out of the plane of the knee joint (Figure 2).

A jig was developed, with the plastic knee, to enable the transepicondylar pin to be utilized as the center of motion. A brace was run down and secured to the femur with a "C-clamp" style bracket going around the patella and attaching to the transepicondylar pin on the other side on the joint (Figures 10 and 11). An additional brace was run to the femur from the bracket to ensure stability. The potentiometers were attached to this jig such that when the knee went from the fully extended position to the fully flexed position, the Z

translational potentiometer contracted and the X and Y translational potentiometers extended to give a positive measurement. By convention, the amount of flexion is measured from zero degrees. Of note, a knee may have a few degrees of hyper-extension. The translational potentiometers were placed along the x, y, and z axes as described earlier. The rotational potentiometers were placed at the tips of the translational ones. As placed, counterclockwise rotation about the given axis was taken to be positive motion.

The motion of the worm gear was controlled by a "Velmax controller/driver", to direct the speed of flexion/extension as well as the direction of motion (sliding plate up or down on the worm gear). The potentiometers fed voltage data into a personal computer program, which controlled the rate of output readings. Readings were typically taken at half second intervals throughout the full range of motion. These readings were stored independently into a six column matrix, representing the six degrees of freedom.

The plastic knee joint was known to be smaller than most human knees and to not move as smoothly as a real joint with cartilage and fatty tissue present. Binding was noted, particularly along Z translation, which traveled the farthest. To overcome this problem, a DC servomotor (24V) was attached to the scaffolding to add a small vibration to prevent binding due to natural forces on the potentiometer slide as it moved. This worked quite well at slow speeds, and did not appear to artificially induce any rotation about the Y axis unless a large vibration was added.

Once the test knee was operating as planned without binding, a human knee was prepared and mounted, as described. Although the worm gear drive was mounted on a series of crossbeams, and thus could be portable, it was not adjusted to suit each knee. Rather, to maintain similar test parameters to allow comparisons, care was taken to ensure the K-rods

inserted at both ends of the test specimen were of appropriate length to allow full flexion and extension once mounted in the worm gear.

Weights to simulate the equilibrium or normal knee condition, 20 pound force (9.07 kg; pound force to be represented as #) on the quadriceps (front pulley) and 10# (4.55 kg) each on the hamstrings and gastrosoleus (rear pulleys) were added (Figure 6). The model was then cycled through full motion to ensure proper positioning of the gages, wires, and other equipment. Once this was established, the motion was repeated three times at the normal weight condition and recorded. The weight on the quadriceps was reduced to 10# and the test was repeated three times to simulate a quadriceps-deficient knee joint. The weight was restored to the quadriceps (20#) and the hamstrings and the gastrosoleus were reduced to 5 lbs (2.27 kg) to simulate the hamstrings-deficient condition, and three tests were run and recorded (Table 4.1). Each knee served as its own control.

Condition	GS	HAMS	QUAD
Equilibrium	10	10	20
Quadriceps Deficient	10	10	10
Hamstrings Deficient	5	5	20

Table 4.1

The posterior cruciate ligament (PCL) which was to be studied first, was then cut arthroscopically by the surgeons while the joint was still on the test stand so the same series of tests (equilibrium, quadriceps-deficient and hamstring-

deficient) could be conducted and recorded immediately. Additional testing was done by adding weight to the quadriceps force (up to 80#) to try to recreate the original normal condition motion line. The knee was then removed from the test stand and the PCL was surgically reconstructed by a standard surgical procedure using an 11 mm bone-patellar tendon-bone graft.

The knee was placed back into the test stand and the same tests, in the same order, were conducted. These three conditions were then compared (normal, PCL deficient and PCL reconstructed). (Figure 12) The effect of knee flexion at the time of graft fixation was also studied by comparing the kinematics of the graft fixed at 30° or 90° of knee flexion.

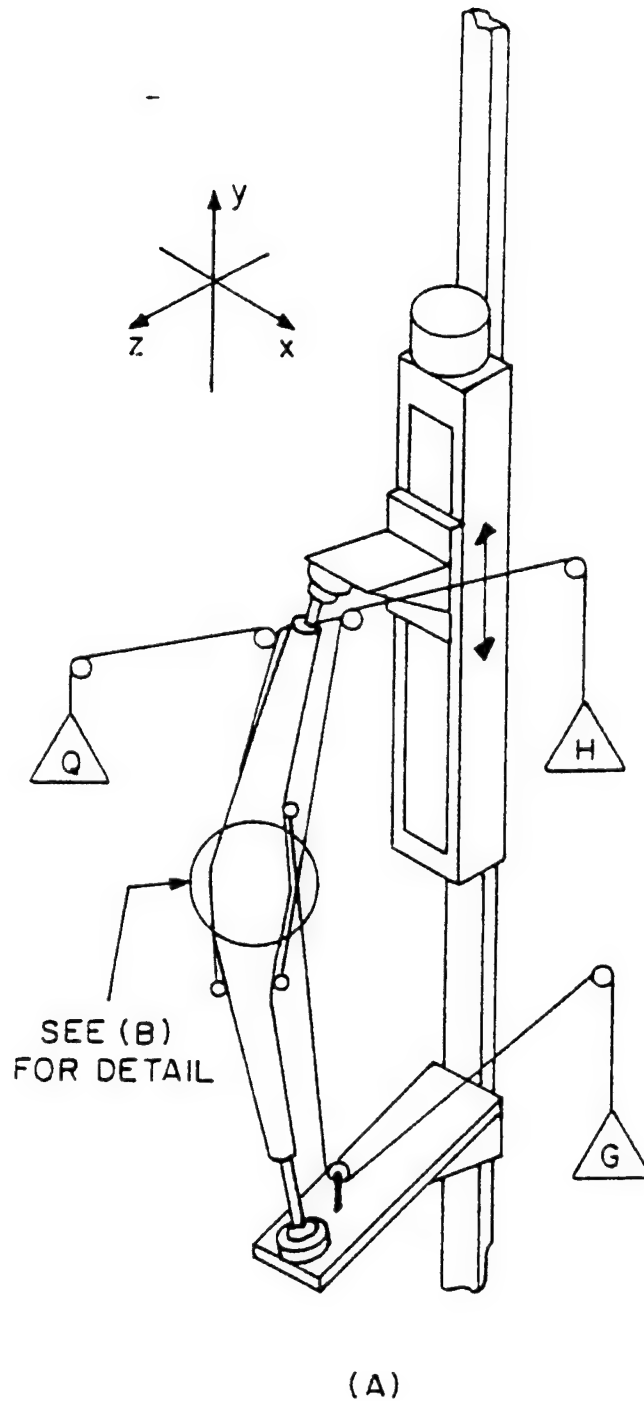


Figure 6: Schematic of the actual test equipment. Use of worm drive slide mechanism is indicated, as well as traction ropes to simulate loading conditions.

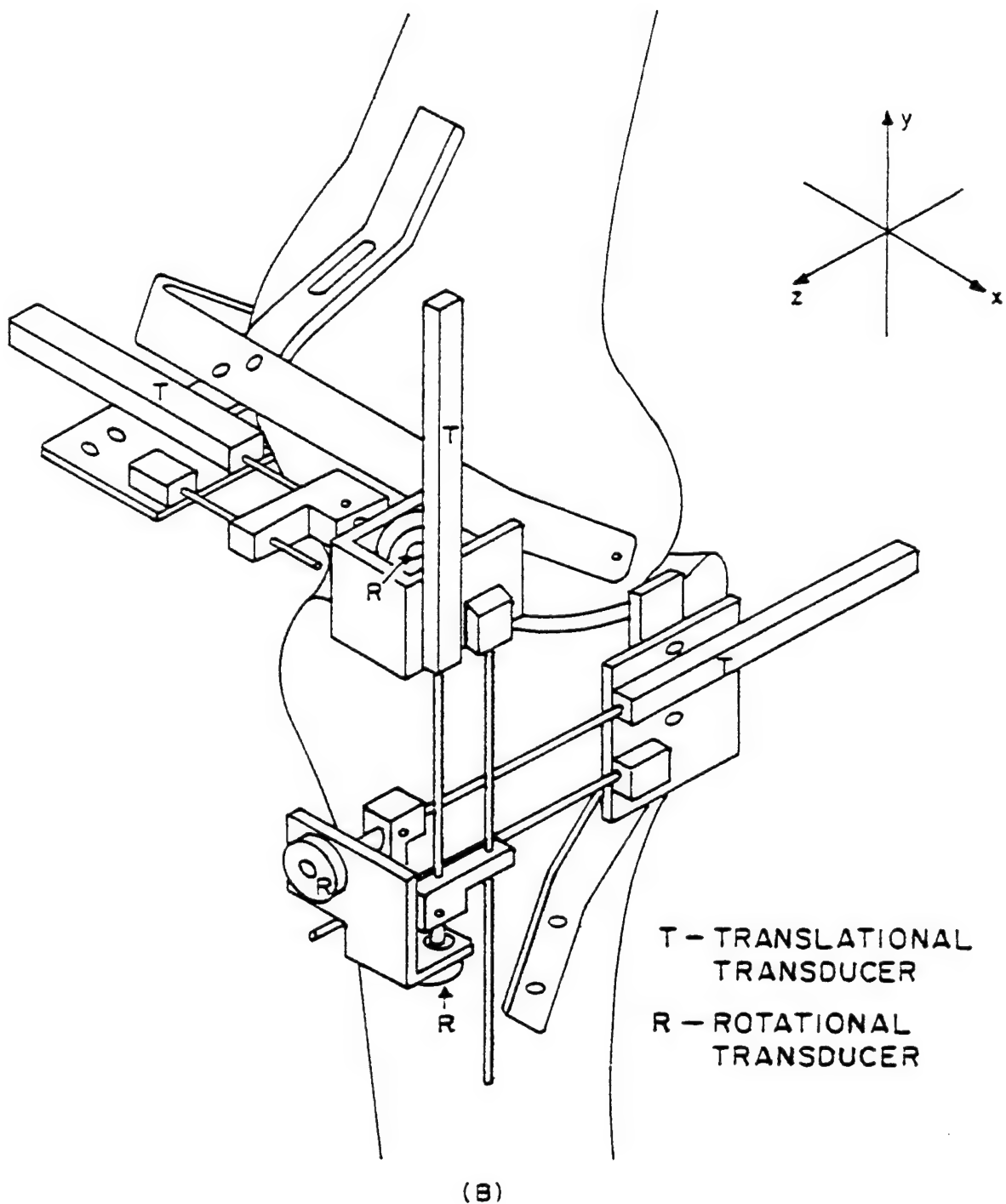


Figure 7: Close-up schematic showing instrumentation.

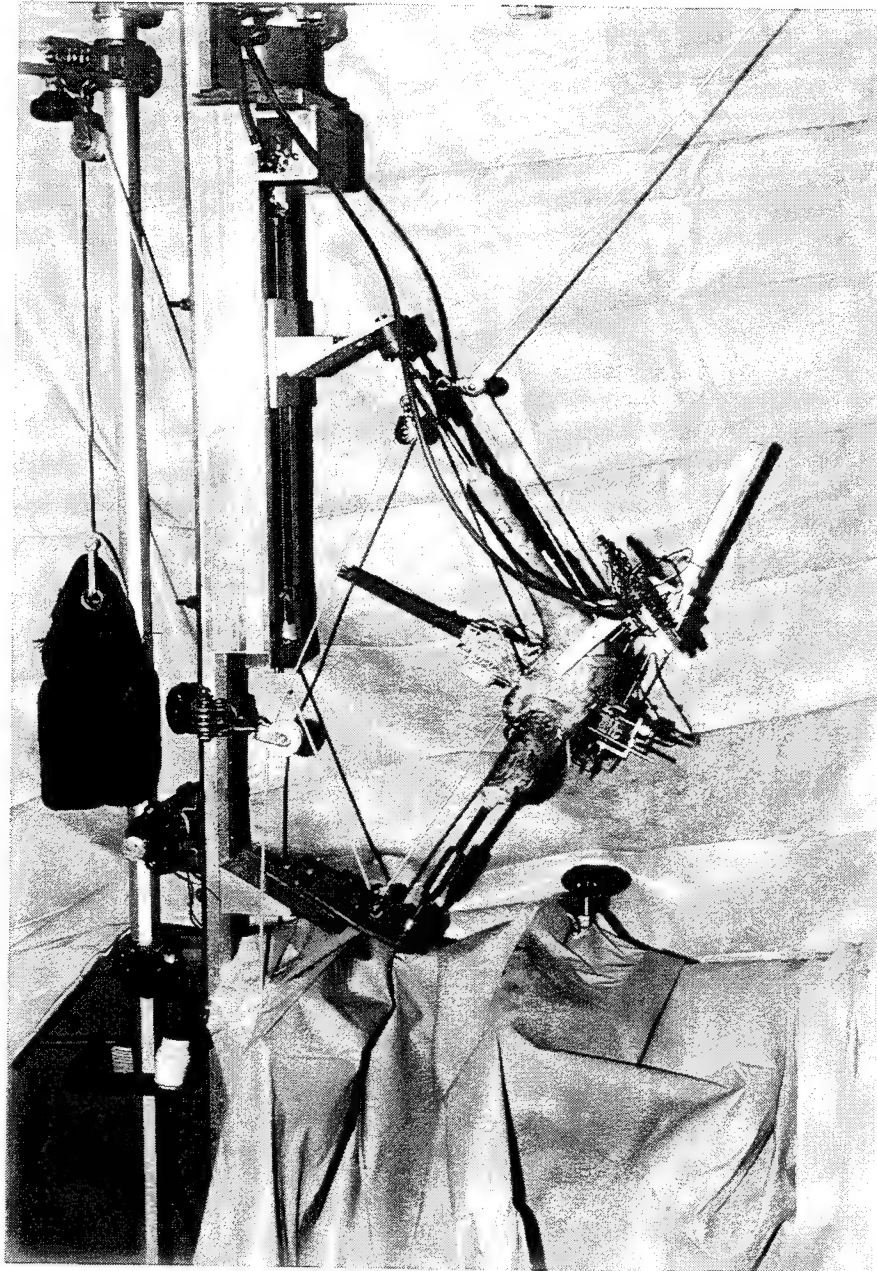


Figure 8: View of human knee in test stand from the opposite side. Note the attachment of the lower ball and socket joint (tibial end) to a plate attached to the framework, while the upper ball and socket joint (femoral end) is attached to the worm drive of the Unislide.

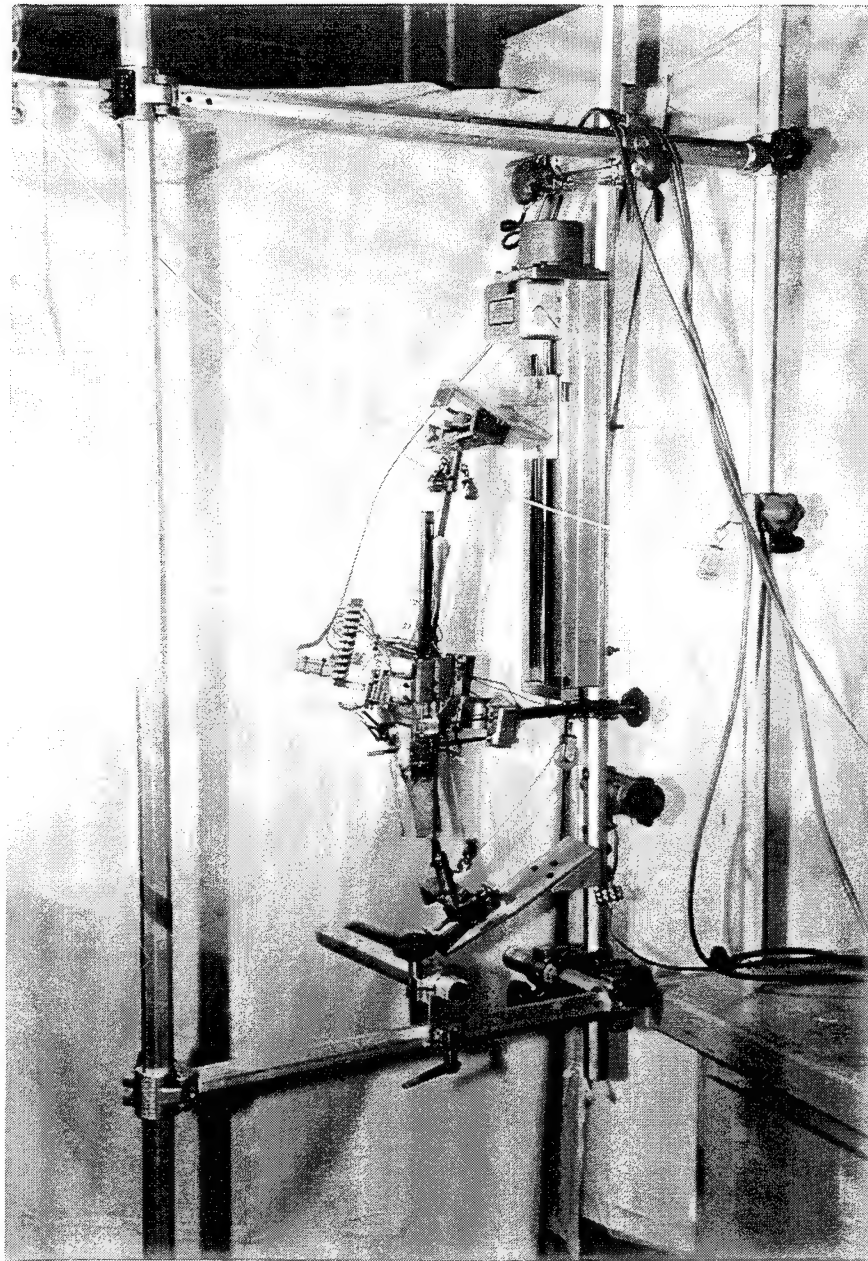


Figure 9: An overall view of the test stand to show the framework used to support the weights as well as equipment. Pulleys are used to help guide the tension ropes.

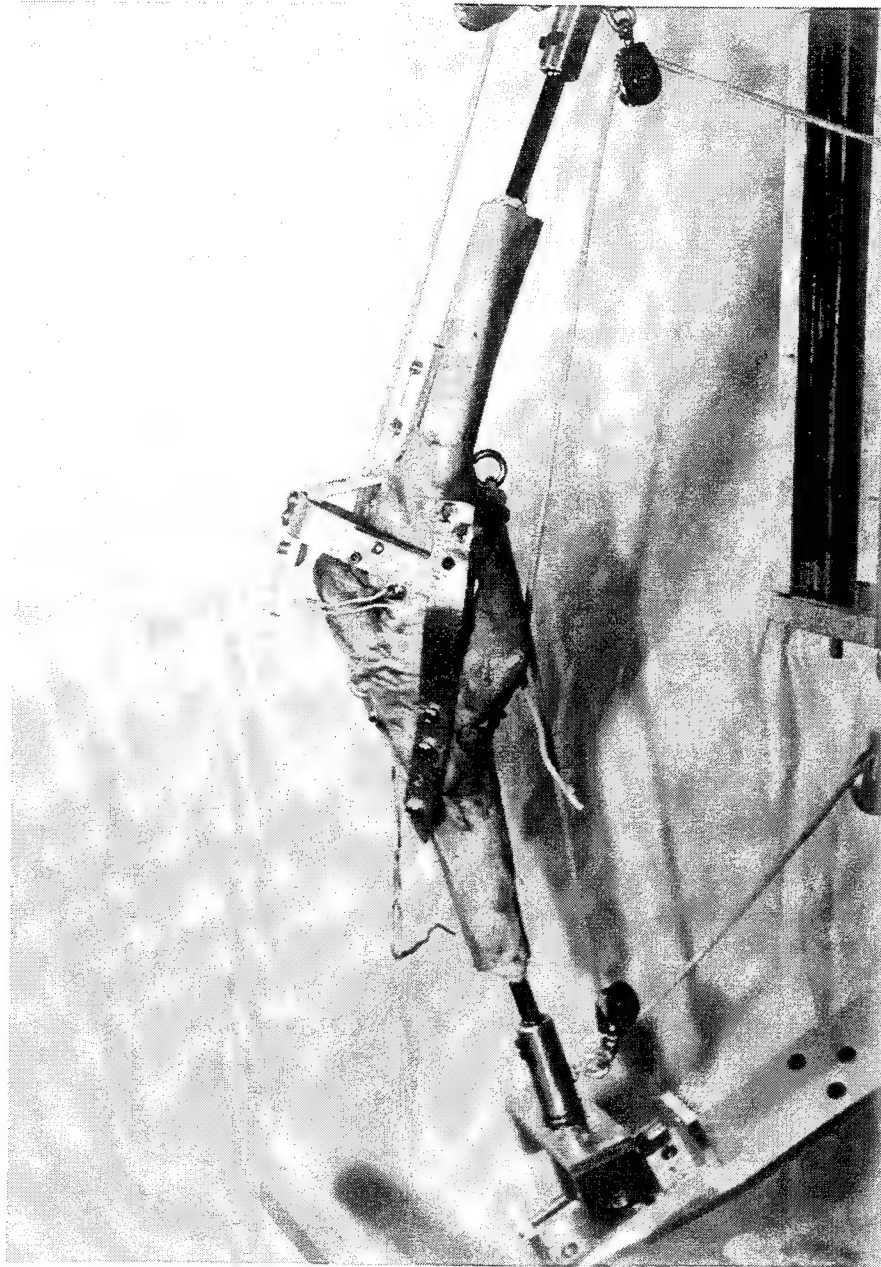


Figure 10: Photograph of a human knee without the test jig in place to emphasize the insertion sites and vector sum points of the simulated muscle forces.

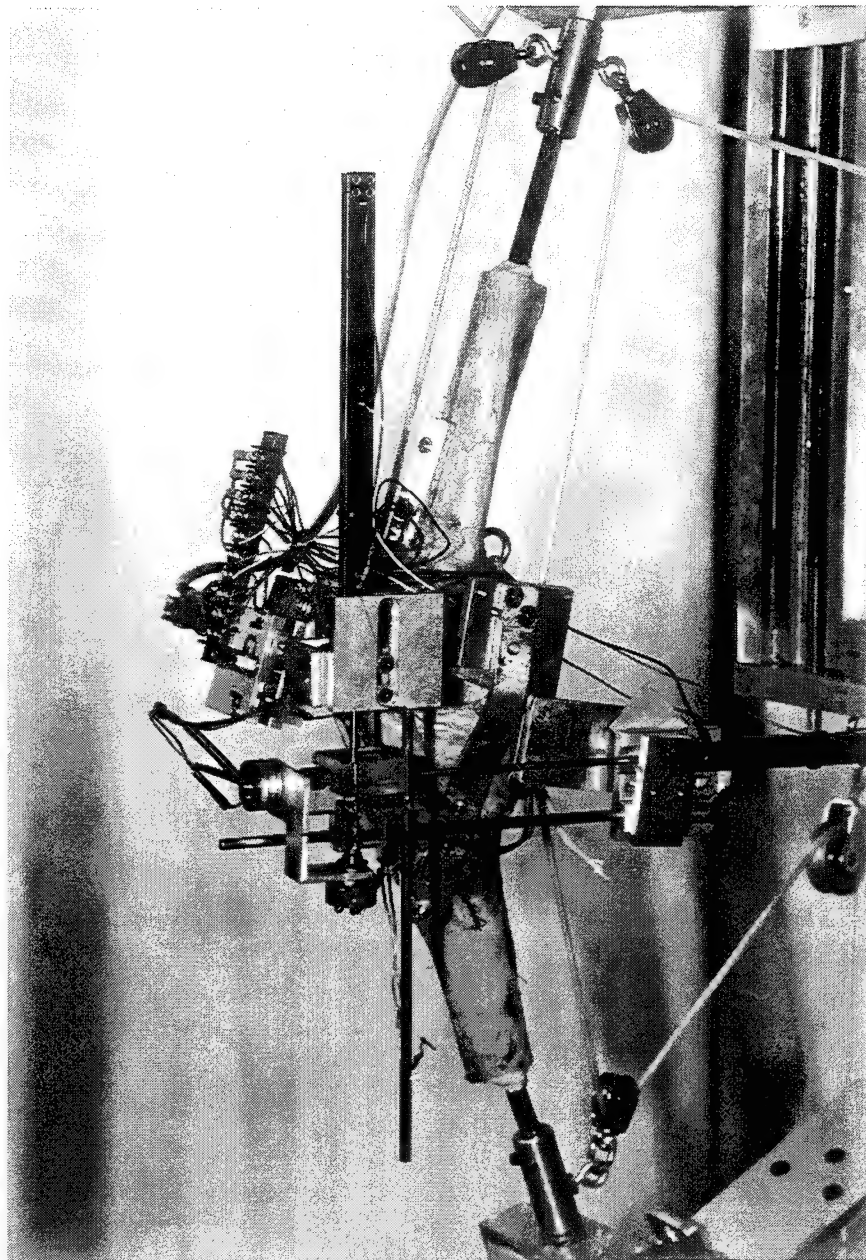


Figure 11: Close-up photograph of the actual jig in place.

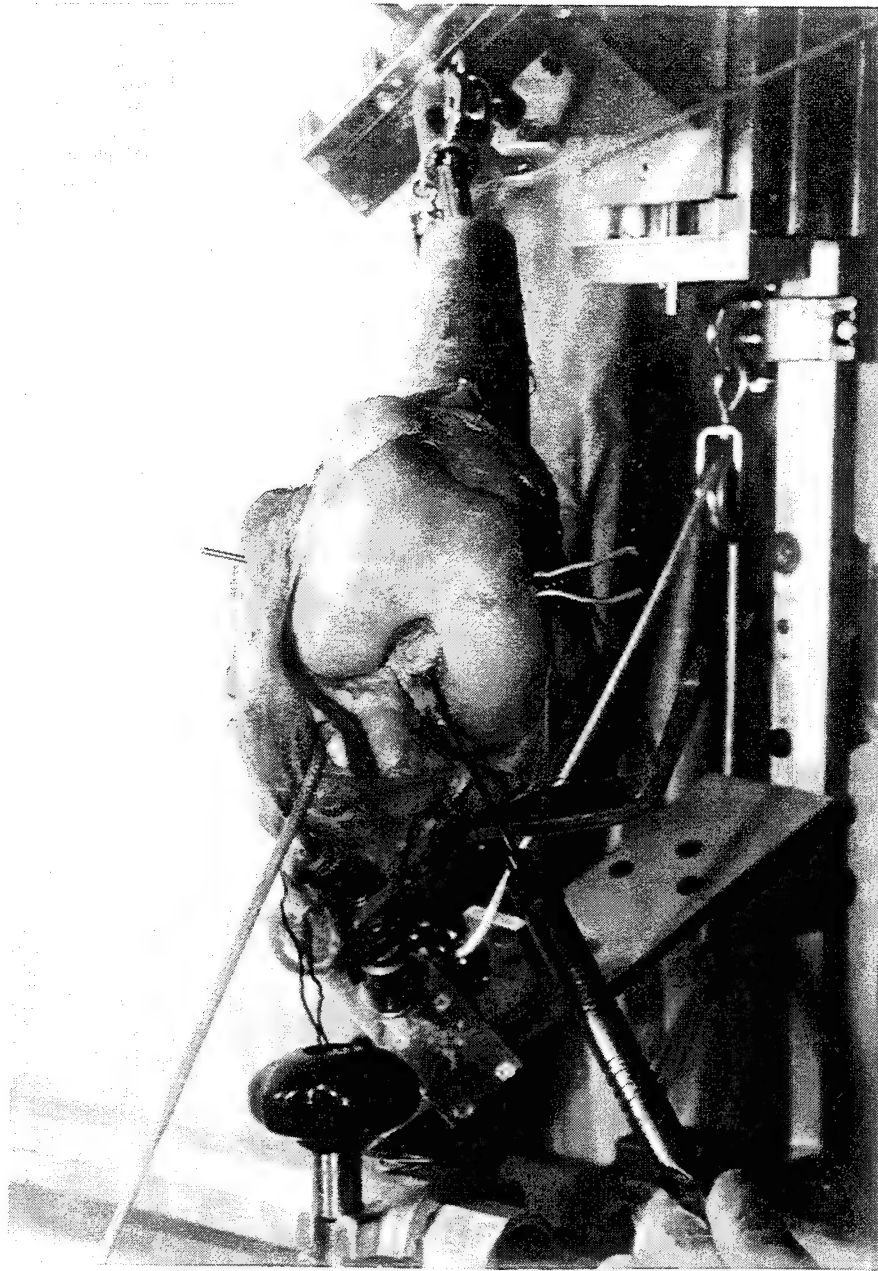


Figure 12: Close-up photograph showing PCL reconstruction.

V. ANALYSIS

A. DATA INTERPRETATION

Five complete human knee joints were used in this study, all prepared as noted previously. The first knee tested (from the female donor) was only used for qualitative comparison. Its main purpose was to test the equipment. Modifications to the test procedure were made until the output obtained reflected biological motion. From there on, minor changes were made to the test stand to ensure proper fit-up of the test knee. Due to the numerous changes undergone at various loading conditions to perfect the test equipment, damage to the ligaments may have occurred, and therefore numerical comparisons with the first knee (Sample 1) were not done.

Before any comparisons could be made, the raw data, read in voltages, had to be converted into degrees and millimeters. Using conversion factors appropriate for the gages being used (22 degrees/volt and 10.685 mm/volt for our set up) a simple MATLAB routine was generated. A consistent zero point was chosen (ensuring the motion of extension to flexion always started at the same point) to allow comparison. A problem was encountered when knee sizes were not exactly the same, causing some knees to travel farther along the Unislide than others to reach the full 110 degrees of flexion desired. This caused the data set to be larger in some instances than others. All four runs differed in size by one to 10 data lines (some due to the range of motion, some due to the method of controlling the data acquisition timing, etc.), so the matrices were plotted together with an appropriate scale change.

With that simple conversion accomplished, various plots were generated. Plots comparing the measured X rotation (always the X axis), verses X, Y, and Z translations and Y and Z rotations were generated. In all samples, plots with similar slopes and features were obtained. The data was found

to be highly repeatable. Figure 13 shows three separate runs from one knee under the same loading conditions, while Figure 14 shows three different knees under the same loading. The minor differences noted in Figure 14 may be explained due to minor changes in actual knee configuration. Since the PCL is known to function as the primary controller in preventing posterior motion of the tibia along the anterior/posterior drawer (Z axis) and external rotation (about the Y axis), the qualities being monitored were focused into these two areas.

Because no two human knees are exactly the same, each knee had its own unique normal condition. This is defined as the PCL intact, with 20# on the quadriceps, and 10# on each the hamstrings and the gastrosoleus. All other conditions were compared to this normal. When the Z translation (Figure 15) and the Y rotation (Figure 16) were plotted for this normal intact configuration, a hysteresis loop was found to occur between the flexion and extension motions. Since there are no other continuous motion models, this had never before been reported. The hysteresis was expected since in a functional knee, reciprocal displacements would be required. (The tibia would need to return to its starting point after a full cycle of motion.) Representative curves documenting hysteresis loops occurring in the X translation (Figure 17), Y translation (Figure 18) and Z rotation (Figure 19) are provided.

After the PCL was severed arthroscopically, thus creating the PCL deficient condition, the curve representing the new condition had a grossly similar shape as the normal condition, but had a different Z translation (Figure 20). This is explained anatomically due to the fact that once the PCL was severed, the posterior drawer was free to shift or drop backward before the knee was flexed, so less translation occurred due to the new zero point.

B. TRANSLATION COMPARISONS

Translation in all three directions (along the x, y, and z axes) were measured and converted via the MATLAB routine to millimeters. The X translation (along the transepecondylar pin) was very minor and determined to be inconsequential, (Figure 17) as was the Y translation (resulting in compression or distraction of the joint, which is minor, as seen in Figure 18). Since the PCL prevents posterior translation at all angles, the Z translation recordings were the major gages used to monitor the progress of testing.¹

For all knees, the trends observed were similar. Once the normal run was established (PCL intact, #20, 10, 10), the succeeding tests were immediately validated against this control run. The data was found to correlate with observed clinical conditions, most of which had not been quantitatively recorded previously. For example, during the quadriceps test, (Figure 21) the quadriceps force of the PCL deficient specimen was increased in 20# increments in an attempt to recreate the normal condition. It was discovered that in comparing the Z translation graphs, the largest differences between the PCL deficient curve and the normal curve occurred at the start and

¹The recorded Z translation was far too great to reflect actual knee motions. The vertical axis scale found on all Z translational graphs represents the actual readings taken, converted into millimeters. This still needs to be corrected for rigid body rotations of the X and Y axes. When this correction was applied, the curves generated demonstrated that from between 30° and 90°, a total absolute translation of @ 25 mm or 1 inch occurs. The same trend is noted in the Y translation curve, presented for hysteresis analysis completeness. The object of this study was to demonstrate consistency among data runs and prove the test equipment. We believe this is demonstrated, since all curves would have to have similar corrections, their position relative to one and another would not change. A change to the design of the test equipment is being done to allow for direct measurements of all motions independently.

end of the half cycle (extension to flexion or flexion to extension), with the deviation found to be the greatest when the knee was at full flexion. The differences decreased with increasing force on the quadriceps, as expected, but approached the normal asymptotically around 70° flexion. Even at high quadriceps loads, the curves remained distinct. The PCL is known to be more functional as the angle of flexion increases, so in a PCL deficient knee (or one where the PCL has been severed) this drop off again from the asymptotic value suggests, since the PCL is not functioning, the posterior translation cannot be corrected by the quadriceps alone.

Specific observations made about the Z translational changes confirm the documented functions of the PCL. Figure 15 shows a hysteresis loop created in one full extension-to flexion-to extension cycle. Once the PCL was severed, the #20, 10, 10 loading condition test was conducted and compared to the normal. The PCL deficient knee shows approximately a 10 mm difference in Z translation in comparison with the normal knee (Figure 20). The quadriceps test confirms that an anteriorly applied force cannot correct for the injury for the entire range of motion. After 70° - 90° , the correction is incomplete (Figure 21).

After the PCL was reconstructed, the Z translation curve shows the shape is similar to the intact normal curve up to 70° of flexion (Figure 22) but the tibia remains posteriorly displaced on the femur. Further, the motion after 70° of flexion is considerably different from the intact state. The curves intersect at two points. This implies that the current reconstruction techniques do not restore normal kinematics.

The normal surgical procedure during reconstruction is to place a pre-load of 20# on the replacement ligament to simulate the forces that would exist in the PCL had it not be damaged. Tests were conducted at three different pre-load

angles, 30° , 45° , and 90° , and no significant differences were found between the three. However, by plotting the reconstructed data versus the normal, we found the reconstructed line crossed over the normal curve at two places, between 70° - 90° flexion (Figure 23). This confirms the suspicion that the anterolateral and posteromedial bands of the PCL act independently and both need to be accounted for at the time of the reconstruction. A new technique involving the use of two different femoral insertion sites will be tested to determine if the reconstructed knee will perform as well as the intact knee.

Even as loading conditions varied, the overall shape and magnitude of the translations were generally similar from knee to knee and condition to condition. The PCL deficient knee curve followed the same path as the normal, but had a different amount of actual translation (Figure 20). Initially, tests were done in the PCL intact state to simulate quadriceps-deficient (#10, 10, 10), as well as, hamstrings-deficient (#20, 5, 5) conditions and these curves turned out to be almost identical. This would indicate that as long as the joint is compressed by external loads and the ligaments are intact, joint surface anatomy is more important than muscle load (Figure 24).

C. ROTATION COMPARISONS

The X rotation is the primary variable being changed, with each knee going from full flexion to approximately 110° flexion. Biologically, Z rotation translates to a knock-kneed or bowlegged condition and was not considered significant for this study (Figure 19 shows a minor rotation @ 4.5 degrees). The Y rotation would place a twist or torque on the knee, which would yield an artificial Z translation, therefore its impact was reviewed.

The overall pattern of the rotations was found to be

repeatable. Y rotation was found to be small compared to X rotation, with an 80% change in the amount of rotation at approximately 90° flexion (Figure 16). It was noted that as the quadriceps force was changed, the zero point displaced. The normal, hamstrings-deficient, and quadriceps-deficient configurations display similar curves, with the hamstrings-deficient curve slightly displaced but rotations the same direction and magnitude (Figure 25, 26, and 27).

The tests done on the PCL deficient knee confirmed that more rotation occurred from 0° to 90° of flexion than did in the intact configuration, further indicating that the PCL is important in controlling external/internal rotation (Figure 28).

Once the PCL was reconstructed, the pattern of rotation was initially opposite that of the intact condition, showing larger magnitudes occurring at smaller degrees of flexion (Figure 29). This suggests that the reconstructed PCL may not have corrected properly for Y rotation, which further implies that the two major bands operate independently. A comparison of the reconstructed knee and the PCL deficient is shown in Figure 30. The rotation occurring at the three different angles of pre-load (Figure 31) shows no major changes are observed by changing the pre-load angle.

D. JOINT REACTION FORCES

The joint reaction forces on the knee were calculated. First, the reactions at the end point ball joints were calculated (Figure 32). After measuring:

L_f - length of the femur, from the femur end of the K-rod to the knee joint

L_t - length of the tibia, from the tibia end of the K-rod to the knee joint

L_g - distance from the femur end of K-rod to the

insertion site of the gastrosoleus force
 L_h - distance from the tibia end of K-rod to the
 insertion site of the hamstrings force
 L_q - distance from the tibia end of K-rod to the
 insertion site of the quadriceps force
 L - length along the straight line connecting the
 end of tibia K-rod to the end of femur K-rod
 X_{rot} - direct measurement of the potentiometers

$$X_{rot} = (\alpha + \beta)$$

$$\gamma = \frac{\pi}{180} (\alpha + \beta) \quad (1)$$

The direct measurement is recorded as a voltage. The
 MATLAB routine converts and stores the voltage to degrees.
 Equation (1) converts the degrees to radians. The following
 forces are either provided for by added weights (F_i) or are
 the horizontal and vertical (x, y) components of forces
 created by the weights and reactions:

Q = simulated quadriceps force
 H = simulated hamstrings force
 G = simulated gastrosoleus force
 Q_x, Q_y = horizontal and vertical components of the
 quadriceps force acting at insertion site
 H_x, H_y = horizontal and vertical components of the
 hamstrings force acting at insertion site
 G_x, G_y = horizontal and vertical components of the
 gastrosoleus force acting at insertion site
 F_x, F_y = horizontal and vertical components of the
 reaction force generated at the femur ball
 and socket joint
 T_x, T_y = horizontal and vertical components of the
 reaction force generated at the tibia ball

and socket joint
 N = resultant force created at the condyles
 simulating the force from the patella

Equations 2-5 represent initial calculations according to simple geometry:

by the cosine law:

$$L = \sqrt{L_f^2 + L_t^2 - 2L_f L_t \cos(\pi - \gamma)} \quad (2)$$

by sine law:

$$\alpha = \sin^{-1} \left[\frac{L_t \sin(\pi - \gamma)}{L} \right] \quad (3)$$

$$\beta = \sin^{-1} \left[\frac{L_f \sin(\pi - \gamma)}{L} \right] \quad (4)$$

perpendicular distance from the line of action of Q to Q-force insertion point:

$$d = (L_t - L_q) \sin \gamma \quad (5)$$

The forces created at the insertion points of the hamstrings weight and the gastrosoleus weight (H and G, respectively), are parallel to the tibia and the femur at full extension. The force created by the quadriceps weight (Q) is broken down into its component forces at the insertion site (Q_x and Q_y) and the reaction force created by the tension cord pushing against the knee (N) is solved for : (Equations 6-8)

$$Q_y = Q \cos \alpha \quad (6)$$

$$N = \frac{Qd}{(L_t - L_q) \cos \beta} \quad (7)$$

$$Q_x = N + Q \sin \alpha \quad (8)$$

Resolution of the component forces yields (Equation set 9):

$$\begin{aligned} G_x &= G \sin \beta \\ G_y &= -G \cos \beta \\ H_x &= H \sin \alpha \\ H_y &= H \cos \alpha \end{aligned} \quad (9)$$

Then the resultant forces at the ends may be solved for, utilizing the summation of forces and moments equalling zero (Equations 10-13):

Σ Moment @ femur ball and socket:

$$\begin{aligned} T_x = \frac{-1}{L} [& Q_x (L - L_q \cos \beta) - Q_y L_q \sin \beta + H_x (L - L_h \cos \beta) \\ & - H_y L_h \sin \beta + N L_f \cos \alpha + G_x L_g \cos \alpha - G_y L_g \sin \alpha] \end{aligned} \quad (10)$$

Σ Forces, x direction:

$$F_x = -(T_x + Q_x + H_x + N + G_x) \quad (11)$$

Σ Moment @ knee joint, along tibia:

$$\begin{aligned} T_y = \frac{-1}{L_t} [& T_x L_t \cot \beta + H_x \cot \beta (L_t - L_h) \\ & + Q_y (L_t - L_q) + Q_x \cot \beta (L_t - L_q) + H_y (L_t - L_h)] \end{aligned} \quad (12)$$

Σ Forces, y direction:

$$F_y = -(T_y + H_y + Q_y + G_y) \quad (13)$$

After solving for the end point reactions (ball and socket forces: F_x , F_y , T_x , T_y) the sum of the forces along the tibia is used to solve for the component joint reaction forces, with forces directed toward the joint (compressive) being considered as positive (Equation set 14):

$$\begin{aligned} J_x &= -(H_x + T_x + Q) \\ J_y &= (G_y + T_y + Q) \end{aligned} \quad (14)$$

From this data, the tibio-femoral joint reaction force, lying along the axis of the tibia, may be calculated through geometry (Equations 15-17):

resulting reaction force J:

$$J = \sqrt{J_x^2 + J_y^2} \quad (15)$$

angle θ created by the resultant and the vertical:

$$\theta = \tan^{-1} \left(\frac{J_x}{J_y} \right) \quad (16)$$

component of the resultant lying along the axis of the tibia:

$$J_t = J \cos (\beta - \theta) \quad (17)$$

In this computation, an assumption is made that the entire force is transmitted through a single contact point between the femur and the tibia at the knee joint. This simplification allows magnitudes of the tibio-femoral reaction force (J) to be determined.

Calculations obtained from the above equations indicate that the tibio-femoral force (along the axis of the tibia) varies directly as the quadriceps force, regardless of the configuration (PCL intact, PCL cut, PCL reconstructed). Table 5.1 provides a summary of the results. Figure 33 is an example of the resulting curve.

The reaction force varies with the quadriceps force. The

same quadriceps force yielded similar results whether the PCL was intact, severed, or reconstructed. The force varies, being initially 1.5 to 4 times the quadriceps force (throughout full range of motion) and decreasing to 1.4 to 2.8 times the quadriceps force as that force reached 80#. All knees have similar behavior patterns, with small deviations. The assumption made considers all forces to act through one point, implying that the net force created at the knee joint would vary as the quadriceps muscle force was changed, but would remain consistent throughout configuration changes to the ACL and PCL. This indicates that when the PCL is cut, the ACL would be required to carry more of the load to keep the net force the same. Since the PCL functions to prevent the tibia from translating posteriorly, a PCL deficient knee is one that has the tibia displaced, up to 25 mm from the Z translation calculations. The ACL would then act as a single point force, along the direction of the long bone.

In all cases after reconstruction, the joint reaction forces were almost the same as the normal, or PCL intact, conditions. The current surgical procedure is adequately providing for the appropriate joint reaction forces.

Sample	PCL INTACT			PCL DEFICIENT			PCL RECONSTRUCTION		
	10*	20*	10*	20*	40*	60*	DEF**	30**	90**
2	18.686	32.008	21.507	28.683	57.659	84.280	32.330	30.865	30.388
	to	to	to	to	to	to	to	to	to
	40.916	67.029	40.914	67.028	119.25	171.47	67.028	67.028	67.028
3	15.609	22.127	14.929	24.445			22.805	21.829	20.662
	to	to	to	to	---	----	to	to	to
	41.912	68.214	41.912	68.214			68.214	68.214	68.214
4	22.558	39.132	24.954	41.979	69.957	95.204	28.493	26.766	30.878
	to	to	to	to	to	to	to	to	to
	42.079	67.549	42.079	67.548	118.49	169.43	67.549	67.549	67.542
5	24.243	42.631	24.576	42.705	82.043	119.24	44.108	42.648	43.188
	to	to	to	to	to	to	to	to	to
	42.448	68.509	42.231	68.508	120.627	172.452	68.509	68.508	68.510

Table 5.1: Joint Reaction Forces

Quadriceps testing was not done on knee 3

* Indicates force applied to simulate quadriceps muscle

** Indicates angle of knee joint at which a 20# force pre-load was applied

Values listed are in pounds, as recorded through the range of motion (full extension to full flexion, back to extension)

DEF - Test was run again at 20# quad force without pre load to recreate PCL cut 20#.

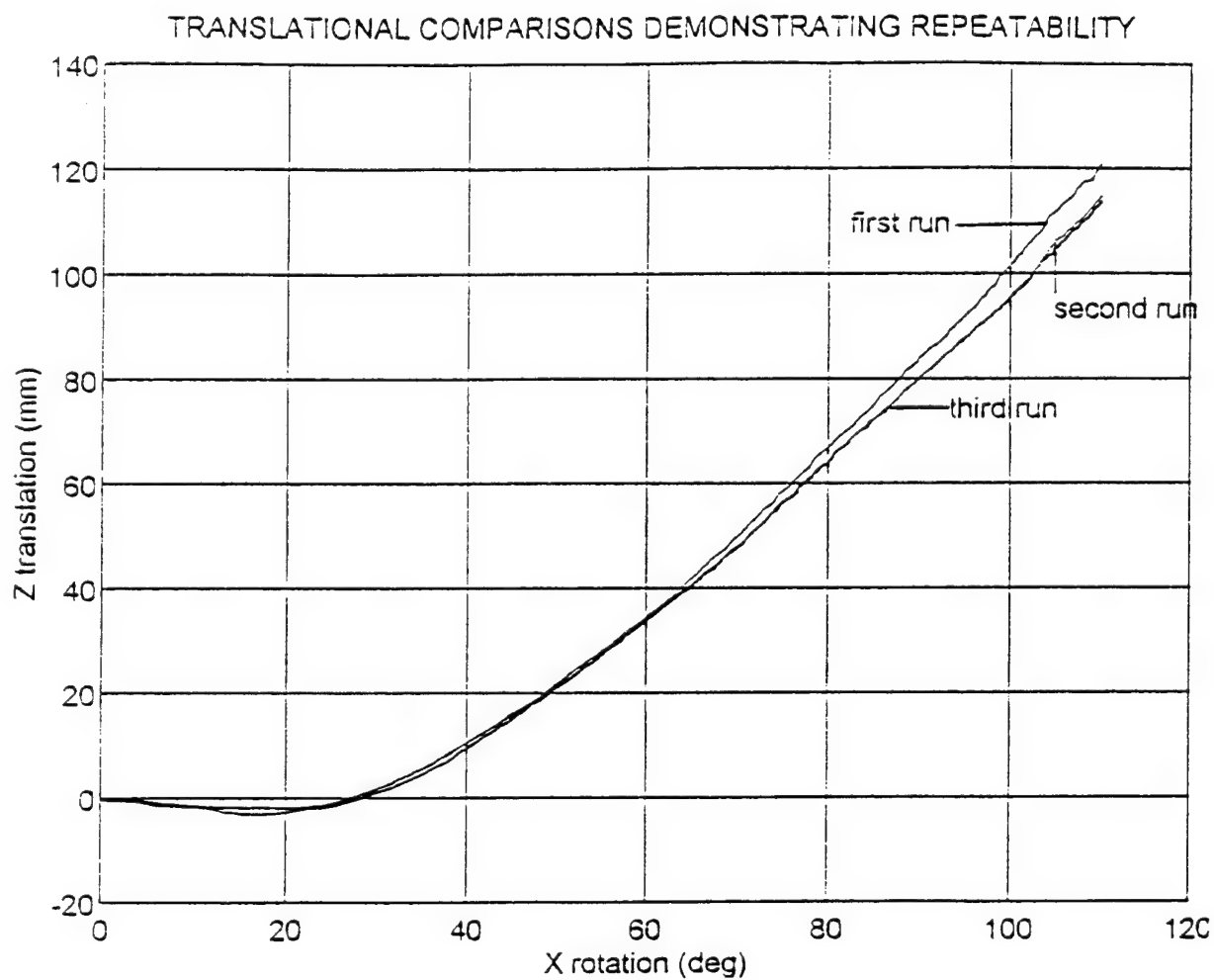


Figure 13: Demonstration of the reproducibility of data runs. Three separate runs from the same knee, normal loading conditions, are shown.

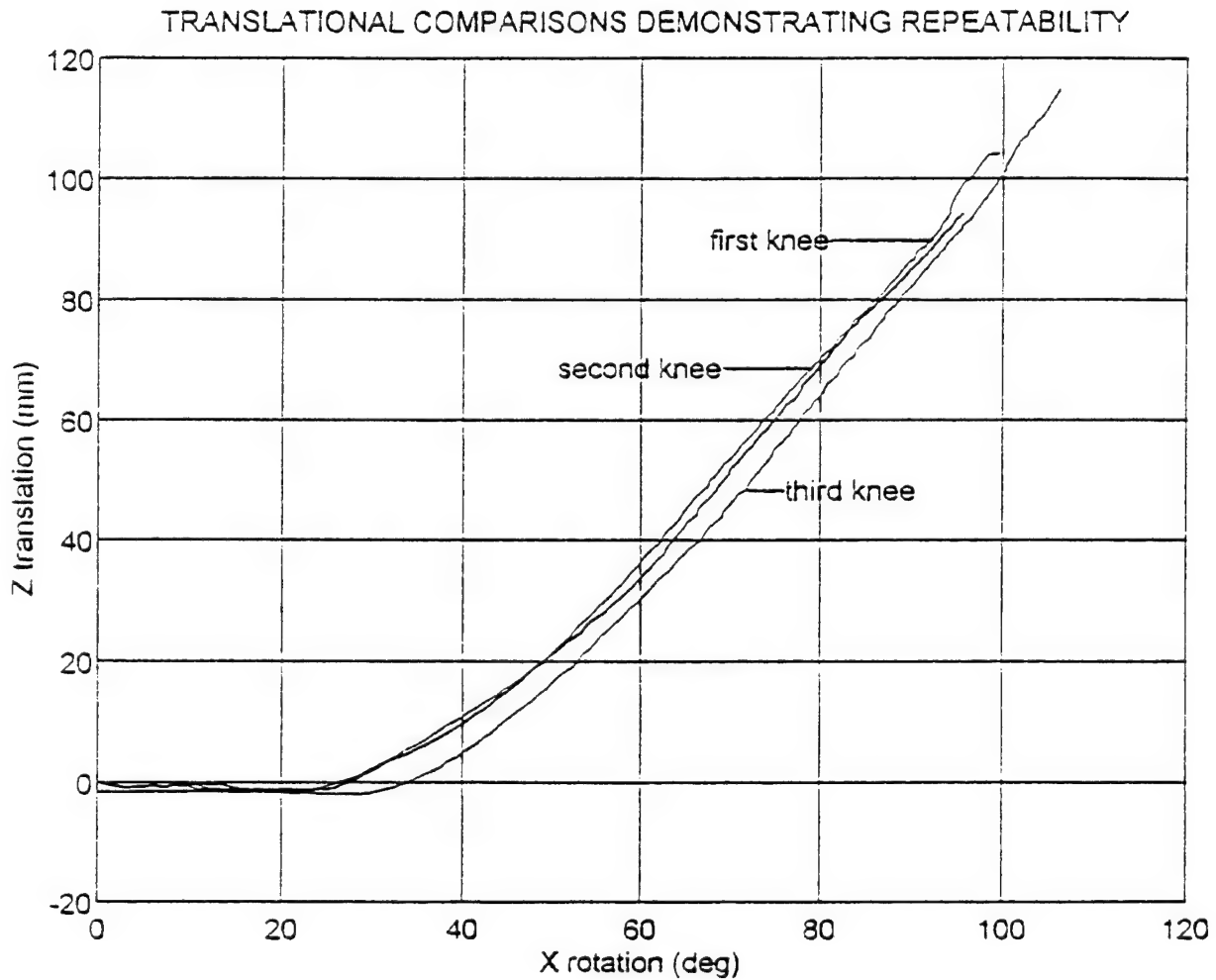


Figure 14: Reproducibility between different knee specimens. Minor deviations are noted, but amount to less than 5 mm. These are easily explained due to individual knee variations.

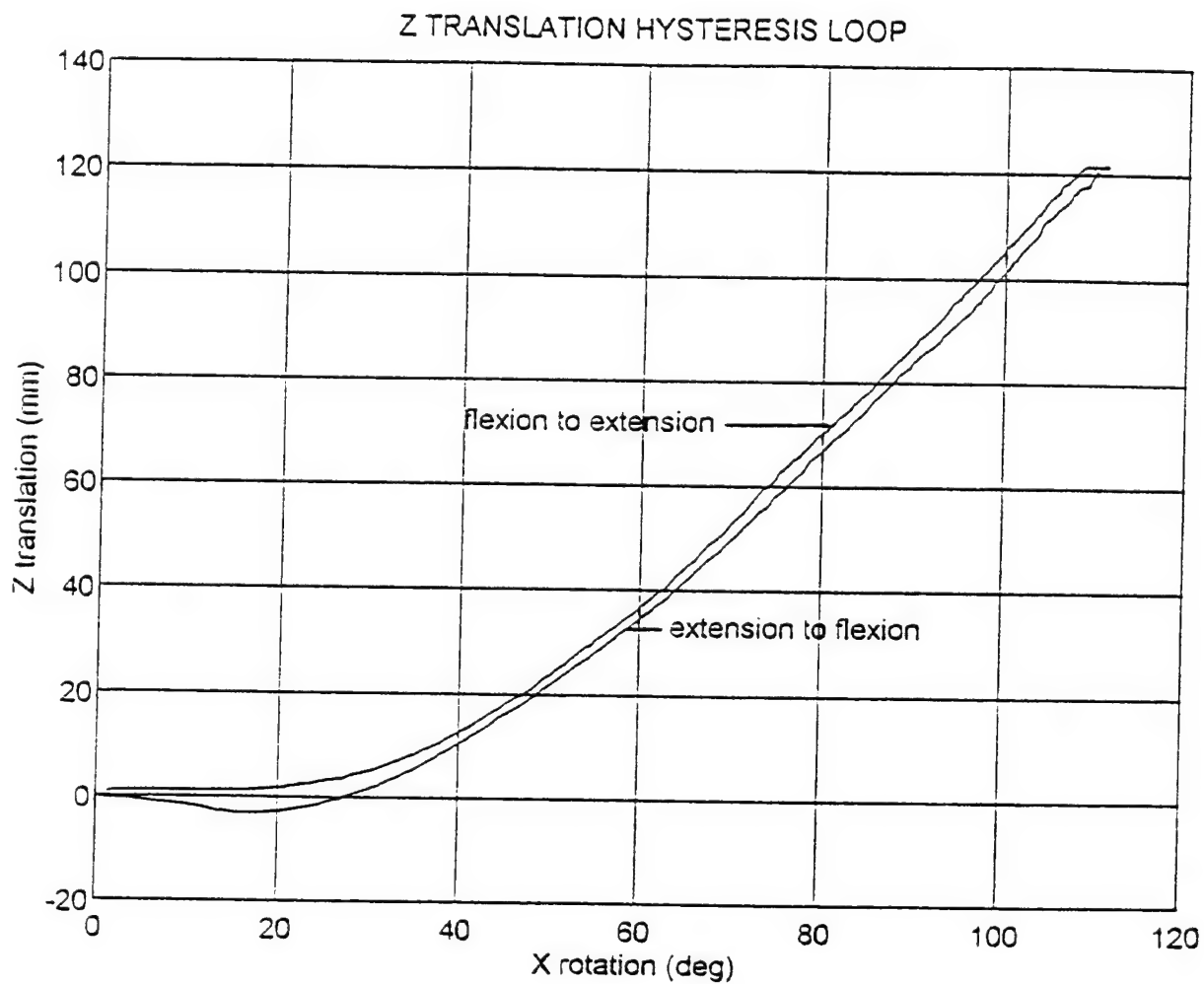


Figure 15: Complete cycle of Z translation, from full extension to full flexion, demonstrating a hysteresis loop, which has never before been recorded.

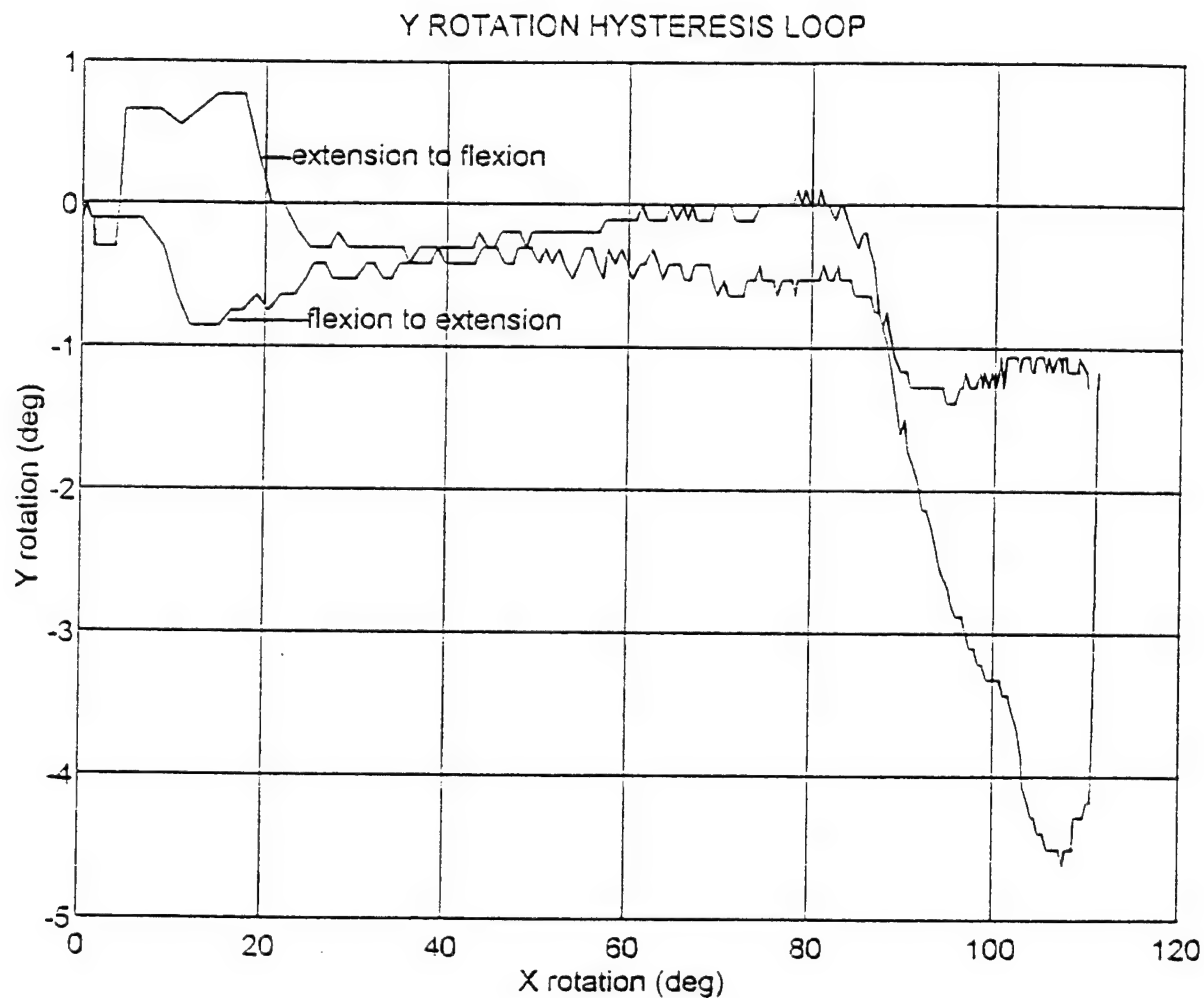


Figure 16: Complete Y rotation recorded throughout continuous motion of full extension to full flexion and back, again showing a hysteresis loop. Notice major change in shape of curve occurs @ 90°, and external rotation occurs.

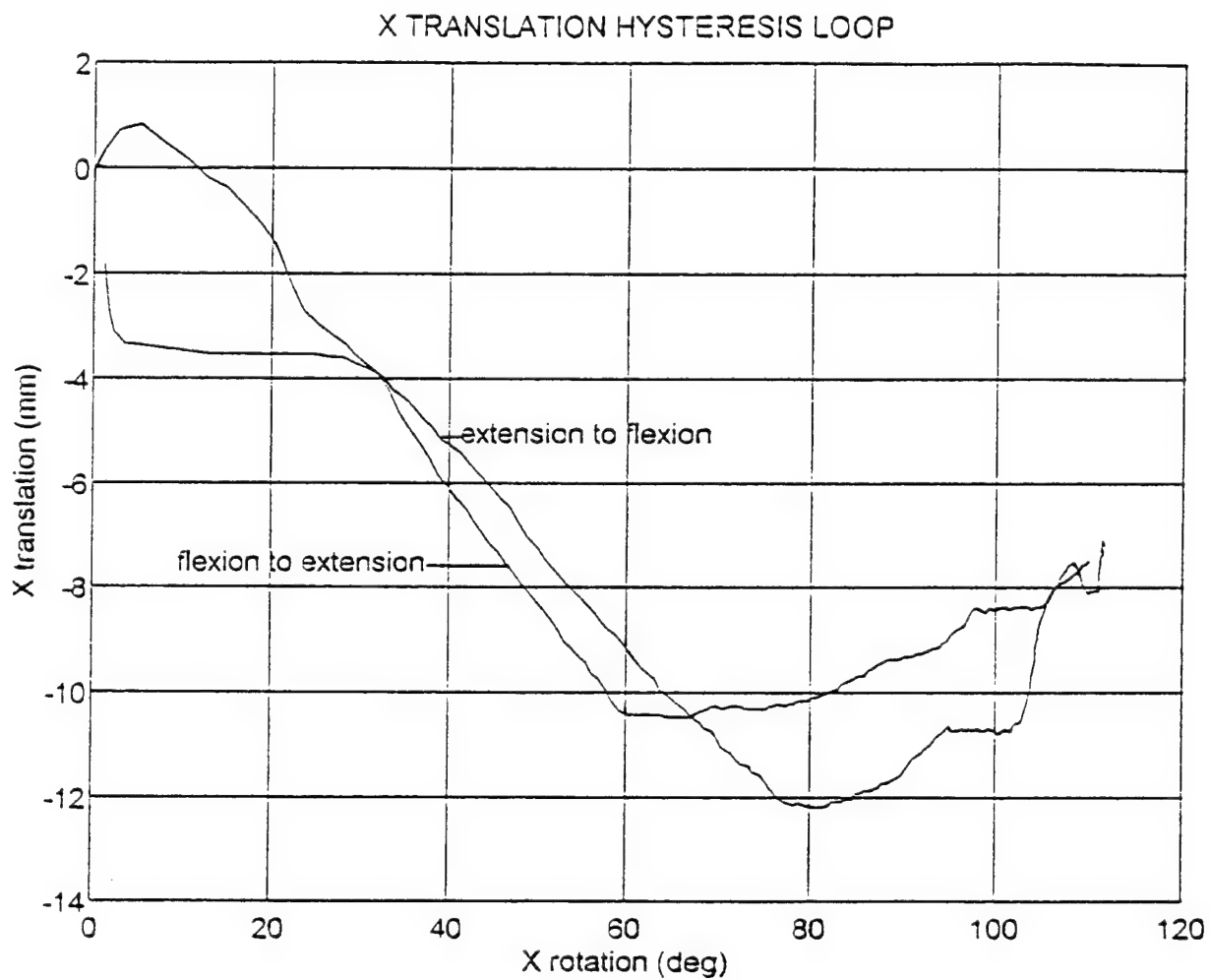


Figure 17: Hysteresis loop of X translation curve.

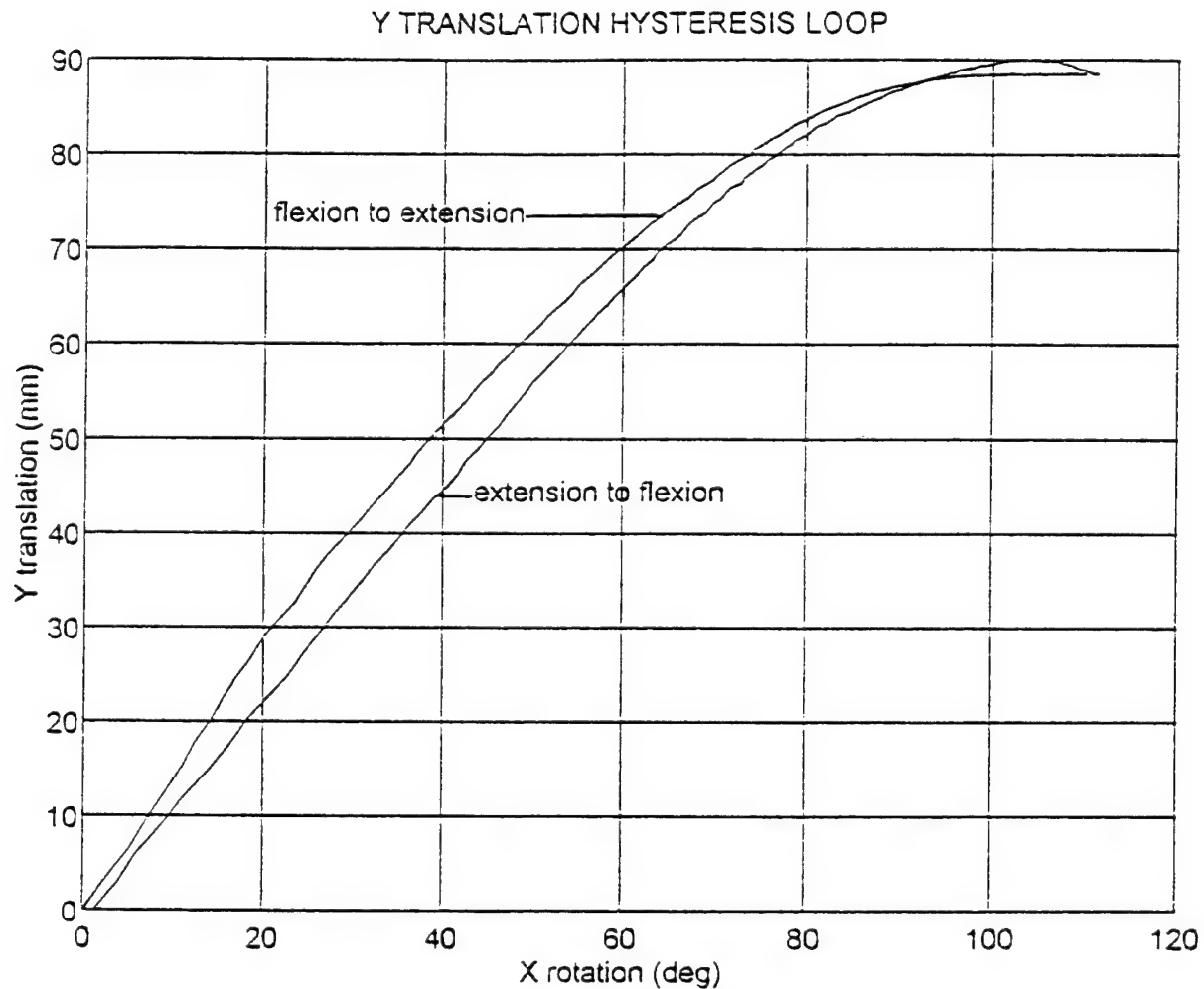


Figure 18: Hysteresis loop of Y translation curve. The Y translation relates biologically to a compression or distraction motion and is known to be small. This curve represents actual recordings of potentiometers and needs to be corrected for X rotation, which is a linear increasing function and will account for most of the Y translation seen.

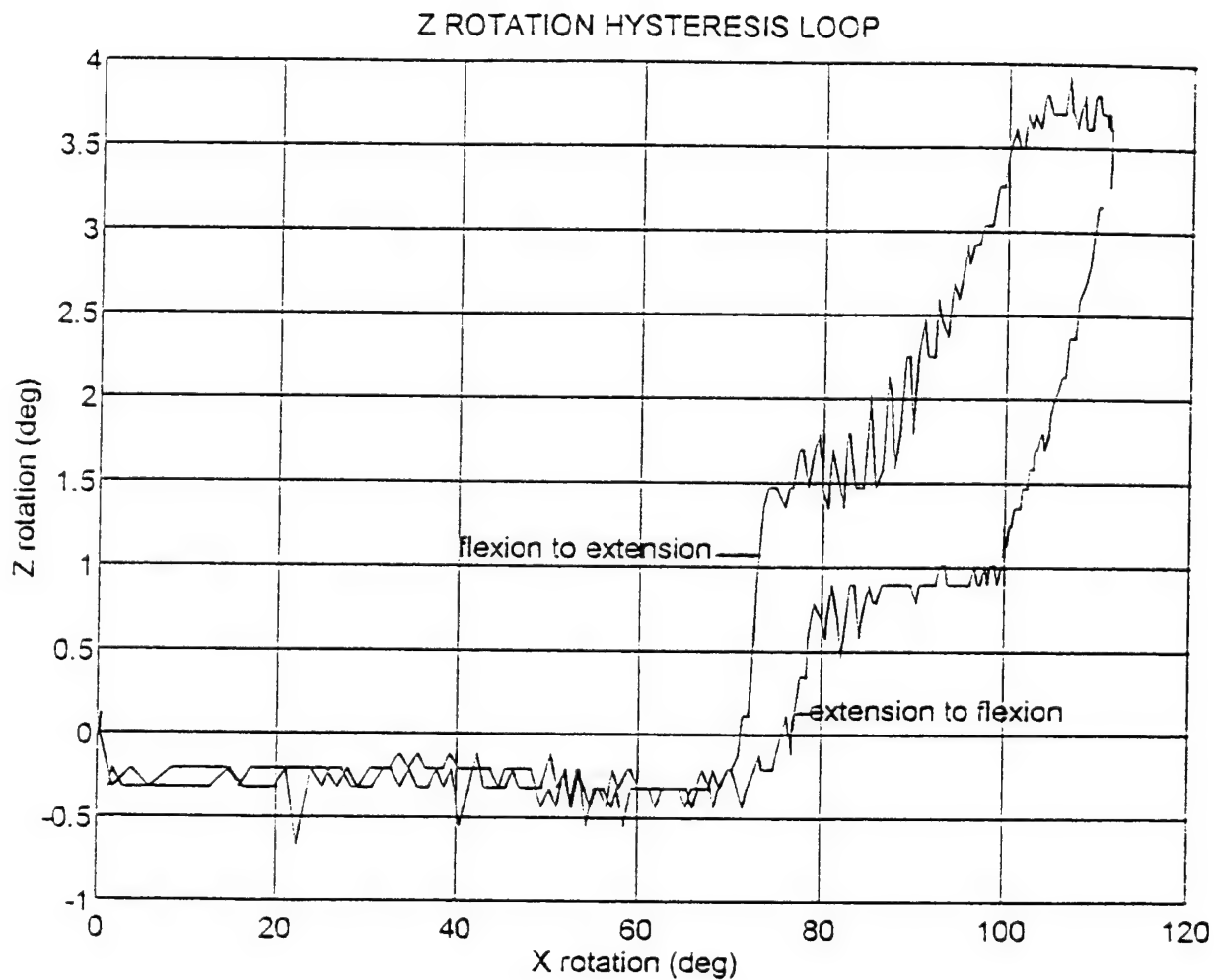


Figure 19: Hysteresis loop of the Z rotation curve. The shape of the curve does not begin to change until @ 70°, where the PCL is believed to exert the most control. Total rotation about the Z axis (abduction/adduction) is shown to be minimal.

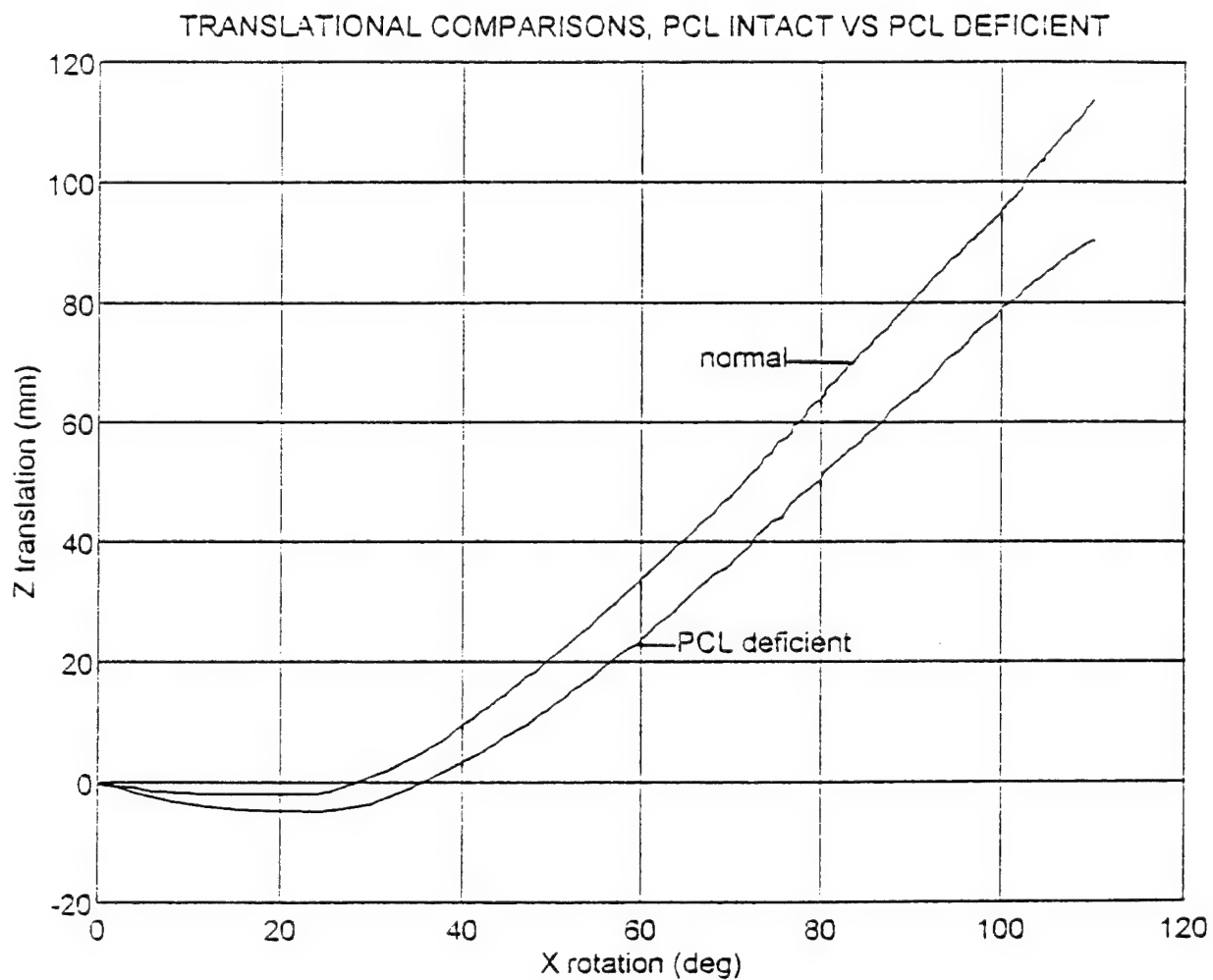


Figure 20: A PCL intact Z translation curve compared to a PCL deficient. The change in translation is expected due to the severed PCL allowing the tibia to shift along the posterior drawer prior to testing.

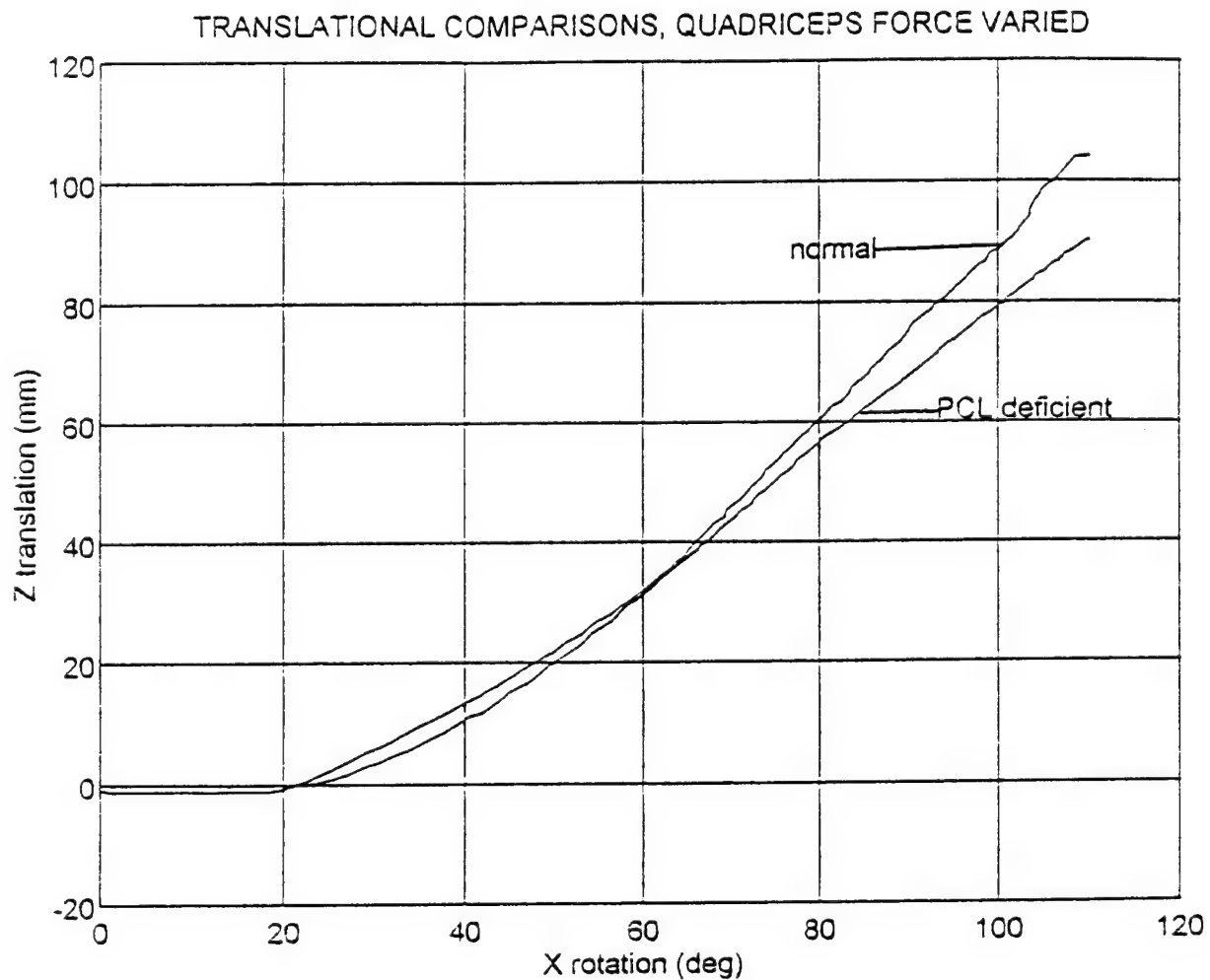


Figure 21: The quadriceps force tested is 80#. Until @ 65°-70°, the curve of the PCL deficient specimen approached that of the normal, then fell off. The PCL is most effective from 70°-90°, and the quadriceps force was unable to recover the normal condition at the higher degrees of rotation.

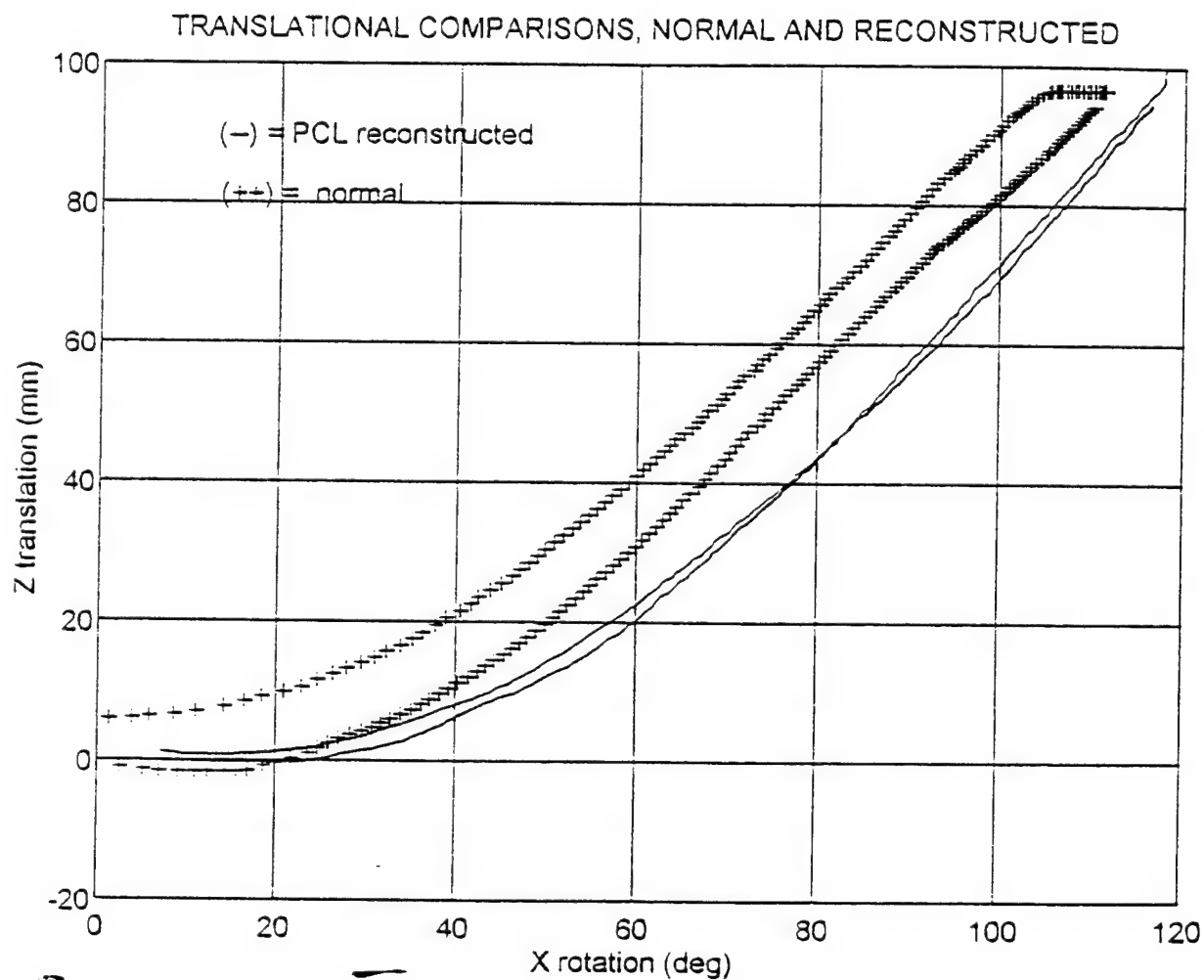


Figure 22: Complete cycle of Z translation motion under reconstruction conditions, compared to the PCL intact specimen. No pre-load is applied. The reconstruction never repeats the intact exactly.

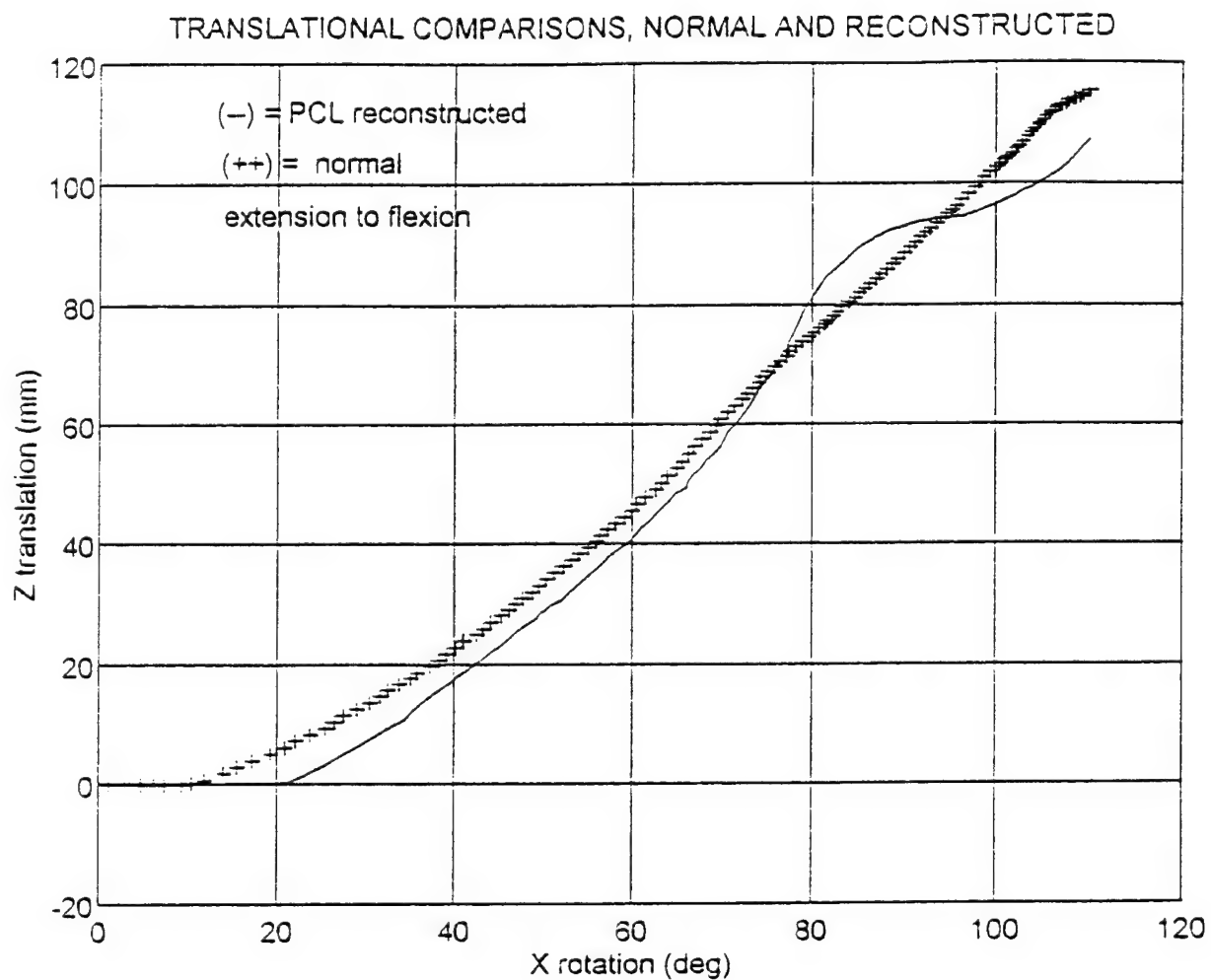


Figure 23: Comparison of the normal knee and the reconstructed knee with a pre-load of 20# at an angle of 90° to simulate the existing quadriceps force. The cross-over between 70° and 90° , demonstrates that both bands of the PCL should be accounted for.

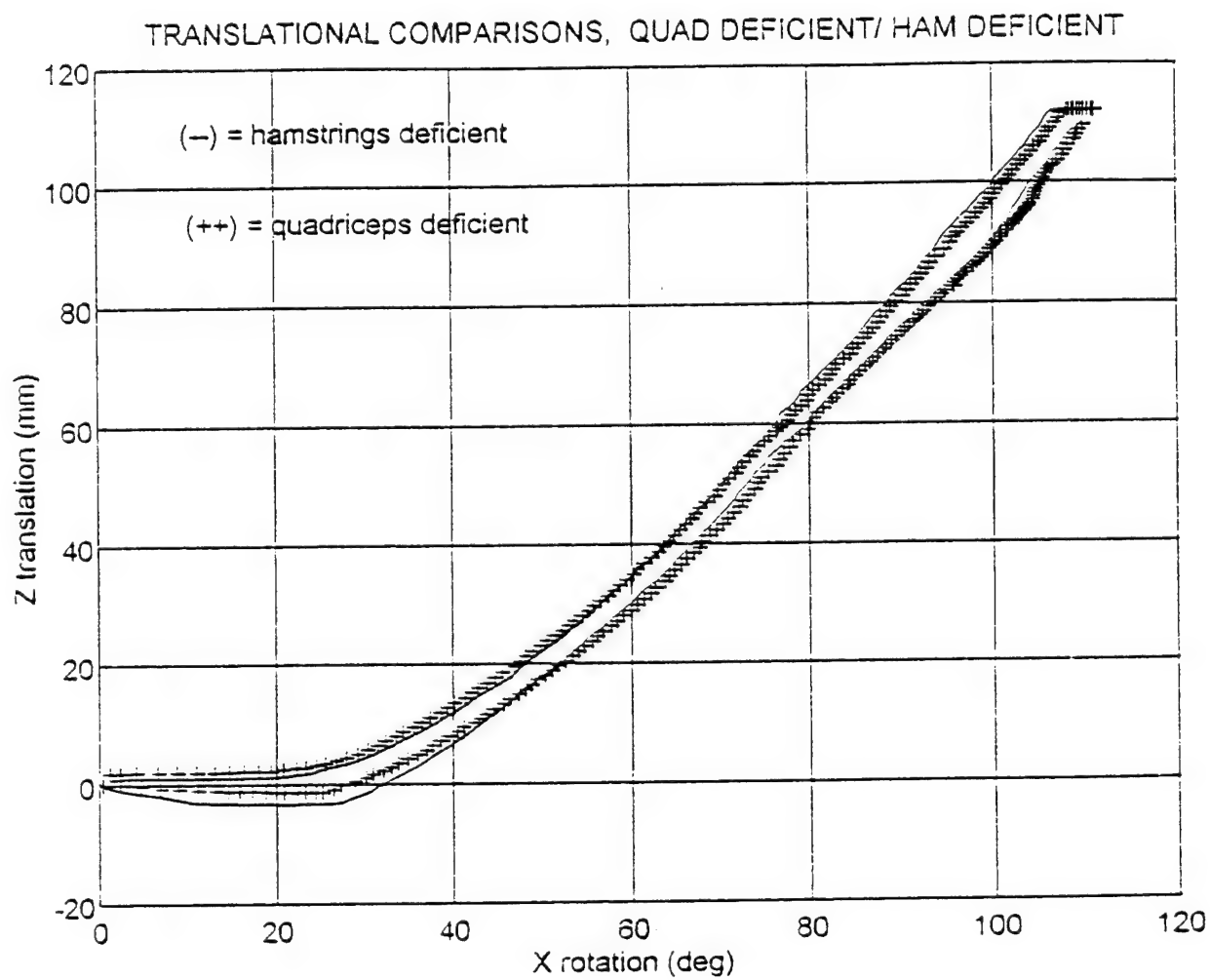


Figure 24: Demonstration that the resulting translations from the hamstrings-deficient and the quadriceps-deficient forces are nearly equal.

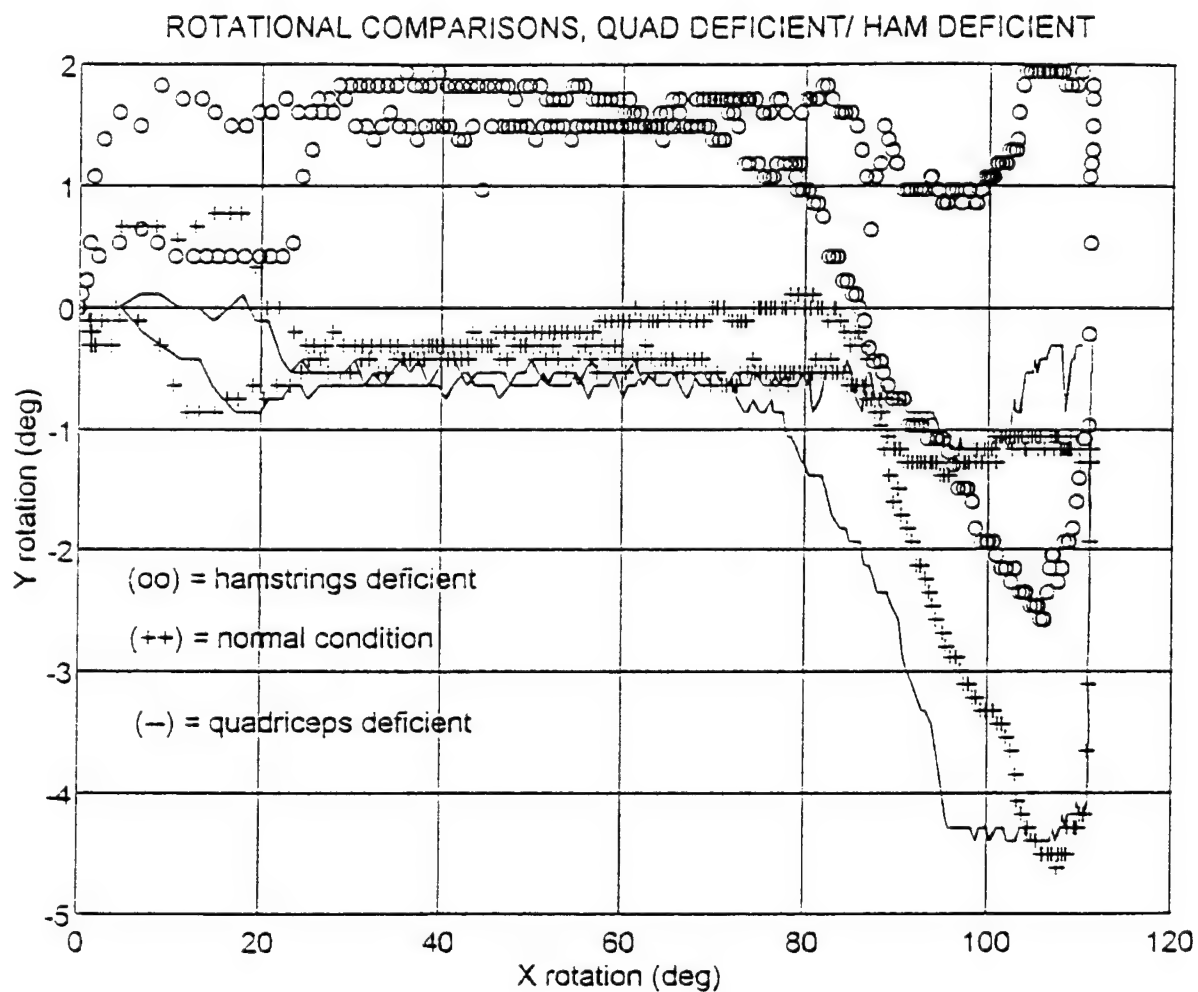


Figure 25: Comparison of Y rotation of the same knee under three different configurations: normal, hamstrings-deficient, and quadriceps-deficient. The curves have the same shape and magnitudes and differ only in initial rotation direction.

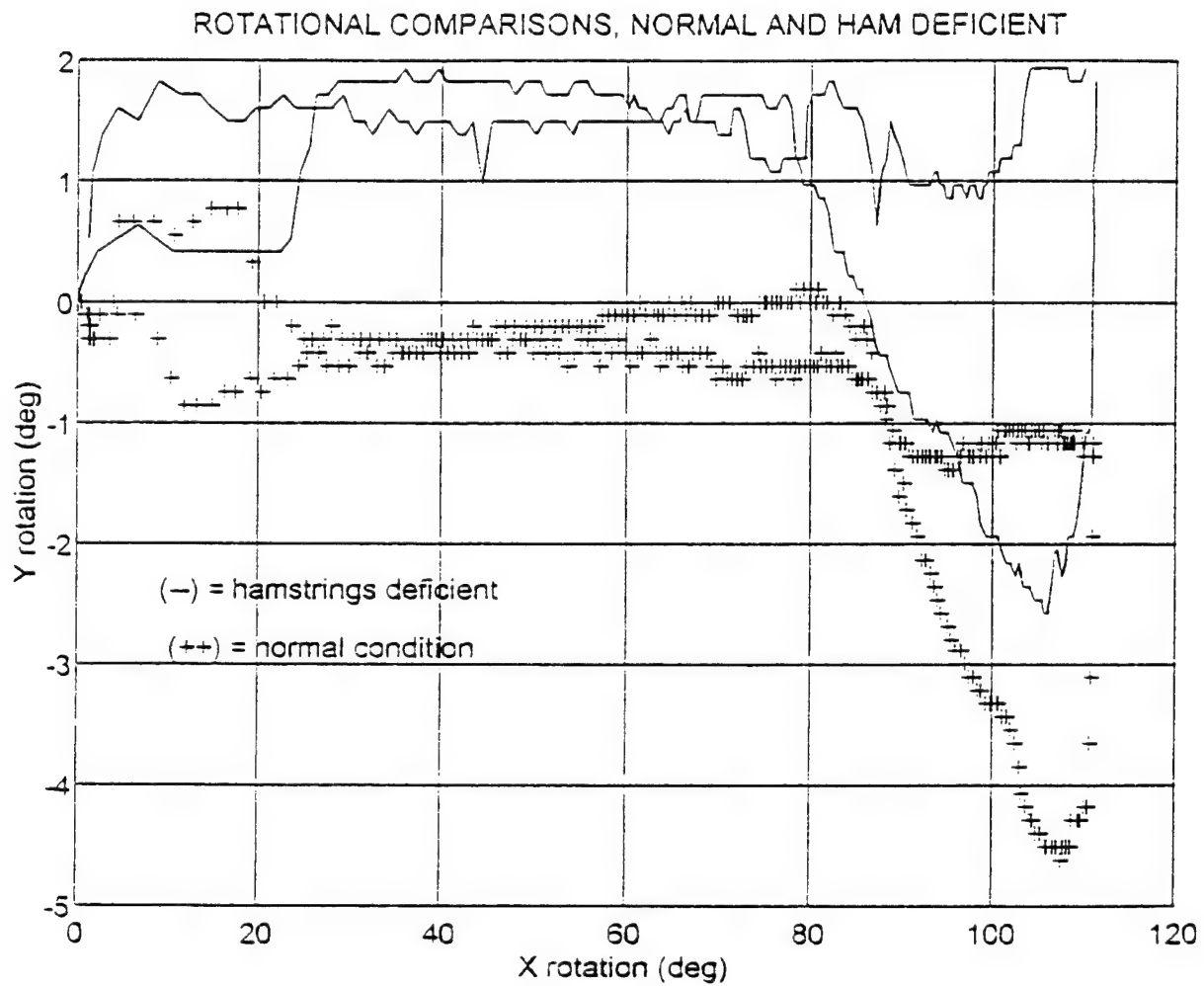


Figure 26: Rotational comparison of the normal configuration and the hamstrings-deficient condition. The curves are the same shape and magnitudes, but are offset by @ 2 degrees.

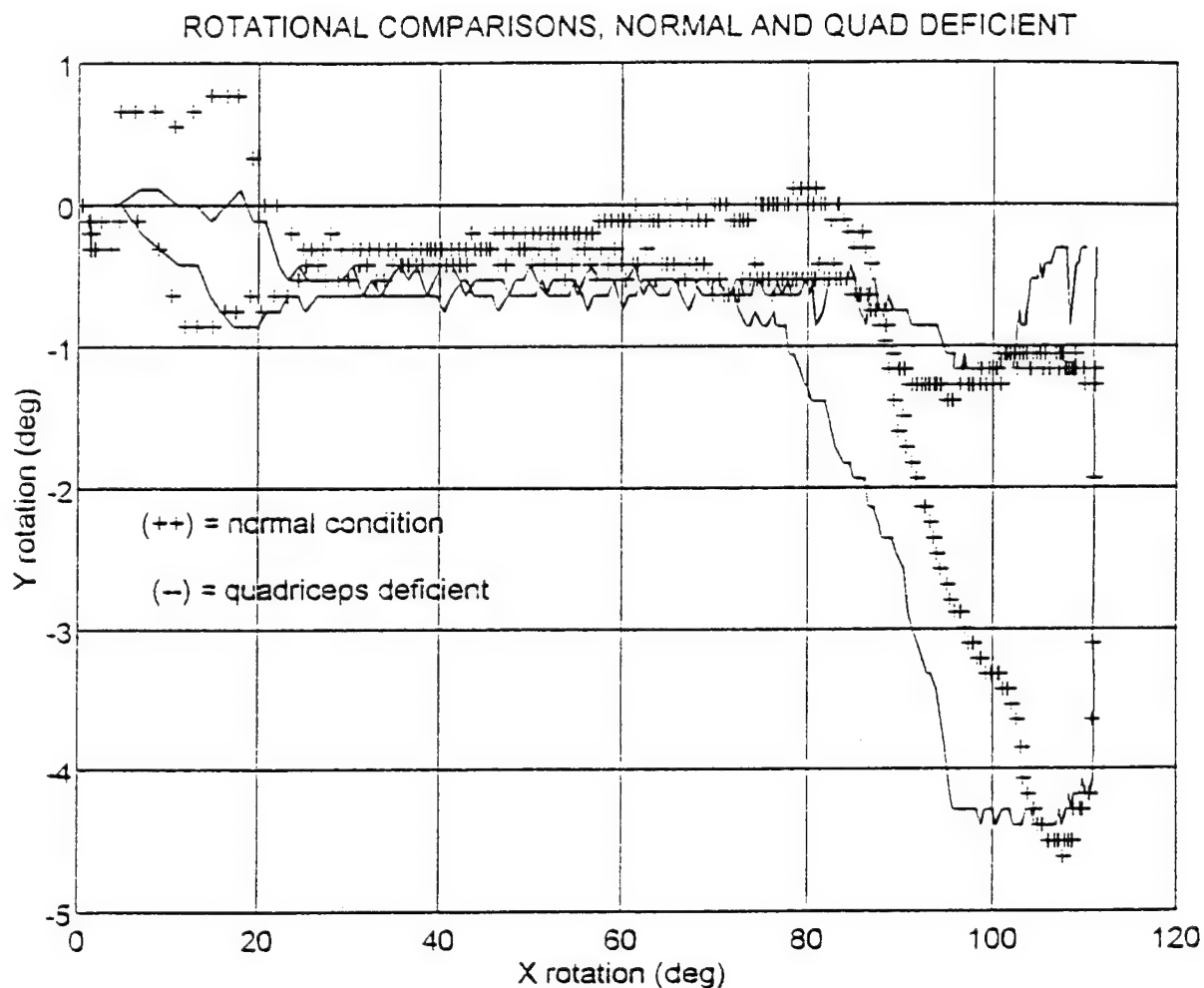


Figure 27: Rotational comparison of the normal configuration and the quadriceps-deficient configuration. The curves are quite similar, with the quadriceps-deficient showing slightly more rotation earlier than the normal.

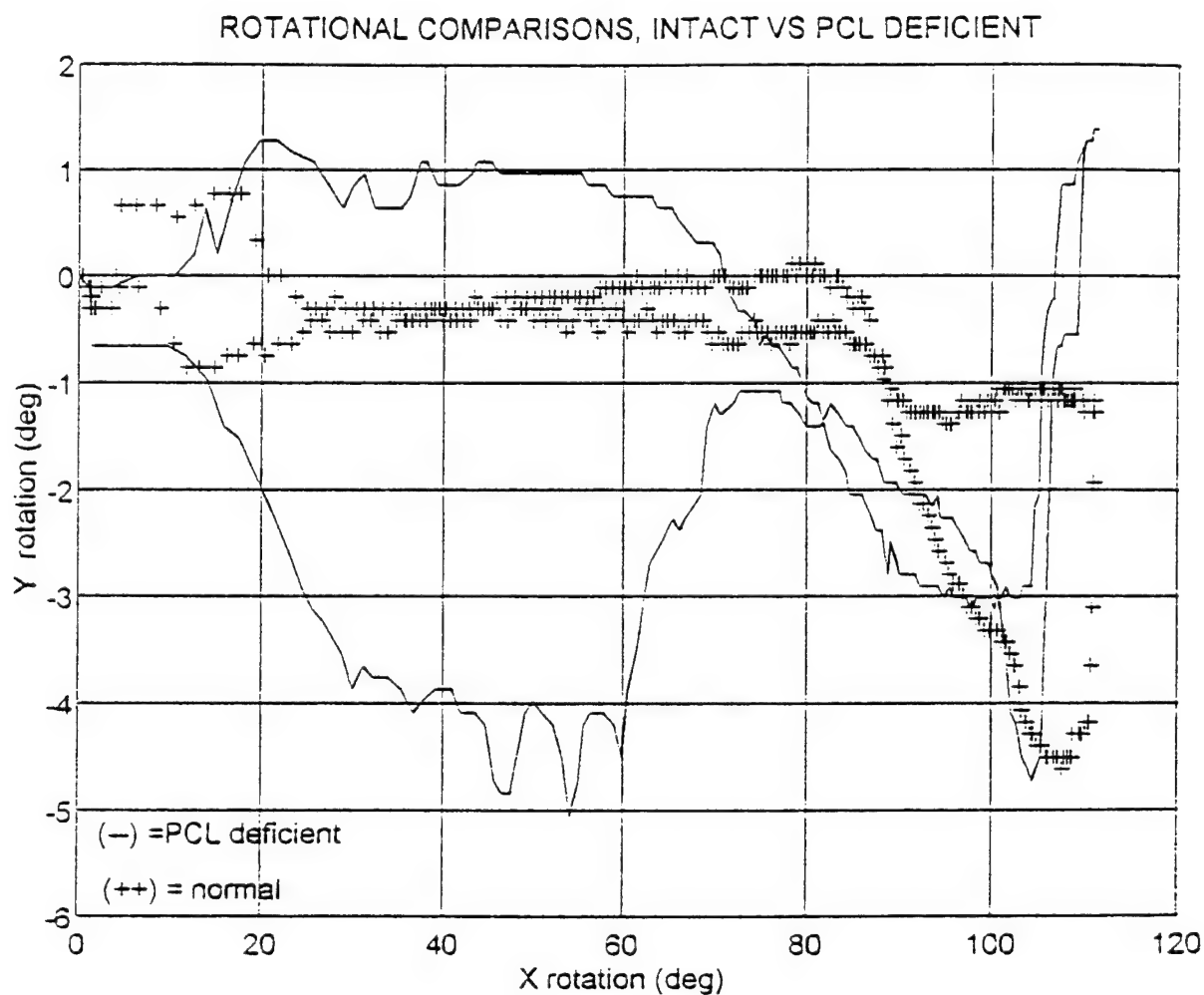


Figure 28: PCL deficient Y rotation curve. With the PCL severed, the tibia is free to rotate externally and internally (varus/valgus motion) as is noted from the drastic change in shape from 20°-70°, differing from the normal. This confirms that the PCL prevents external/internal rotation of the tibia.

ROTATIONAL COMPARISONS, NORMAL VS 90 DEGREE ANGLE OF PRE-LOAD

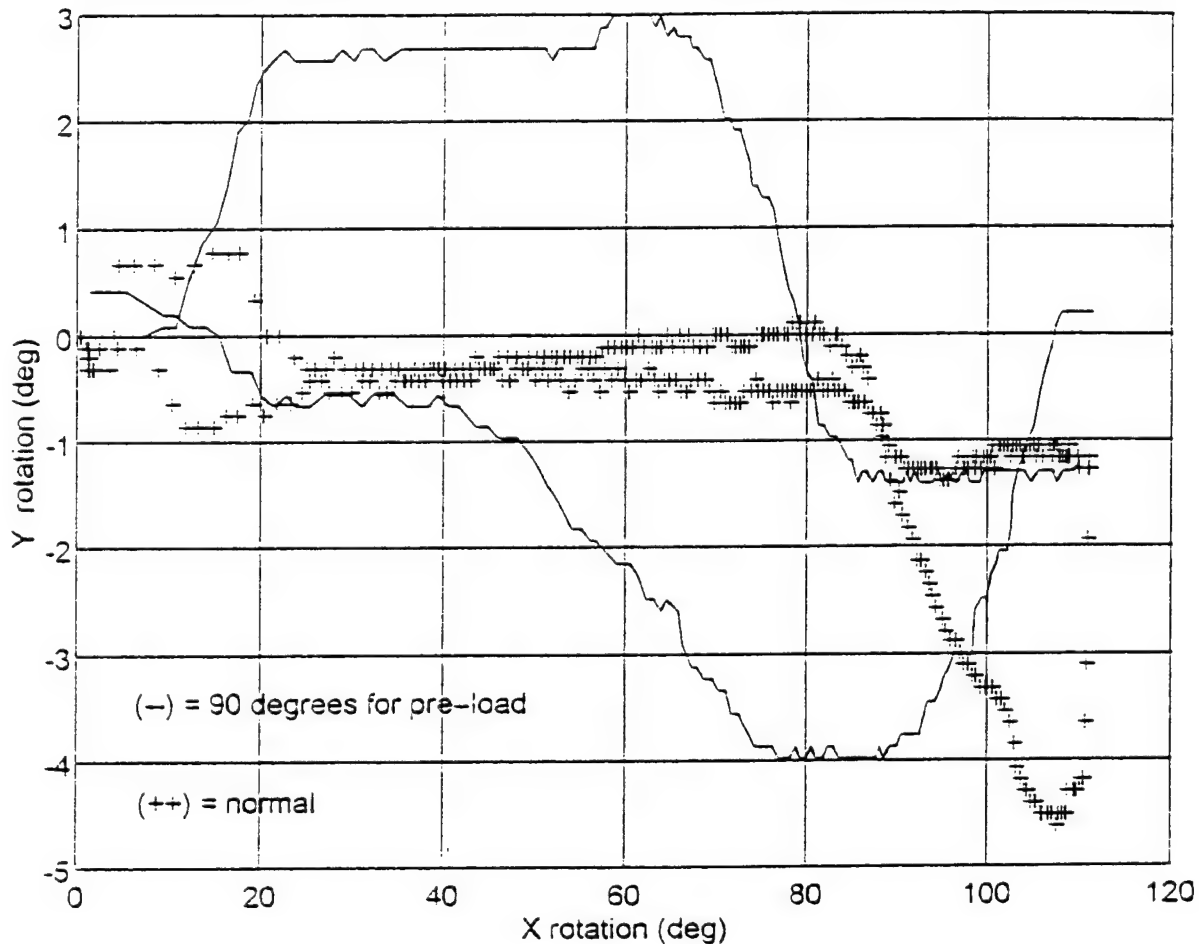


Figure 29: Y rotation of PCL reconstruction with a pre-load of 20# given at 90° flexion, compared to the intact. The lower halves of both curves are similar (although offset by 30-40 degrees). The drastic difference in the upper halves between 20° and 80°, in addition to the curves being similar between 80°-110° indicate that the two bands do need to be accounted for independently.

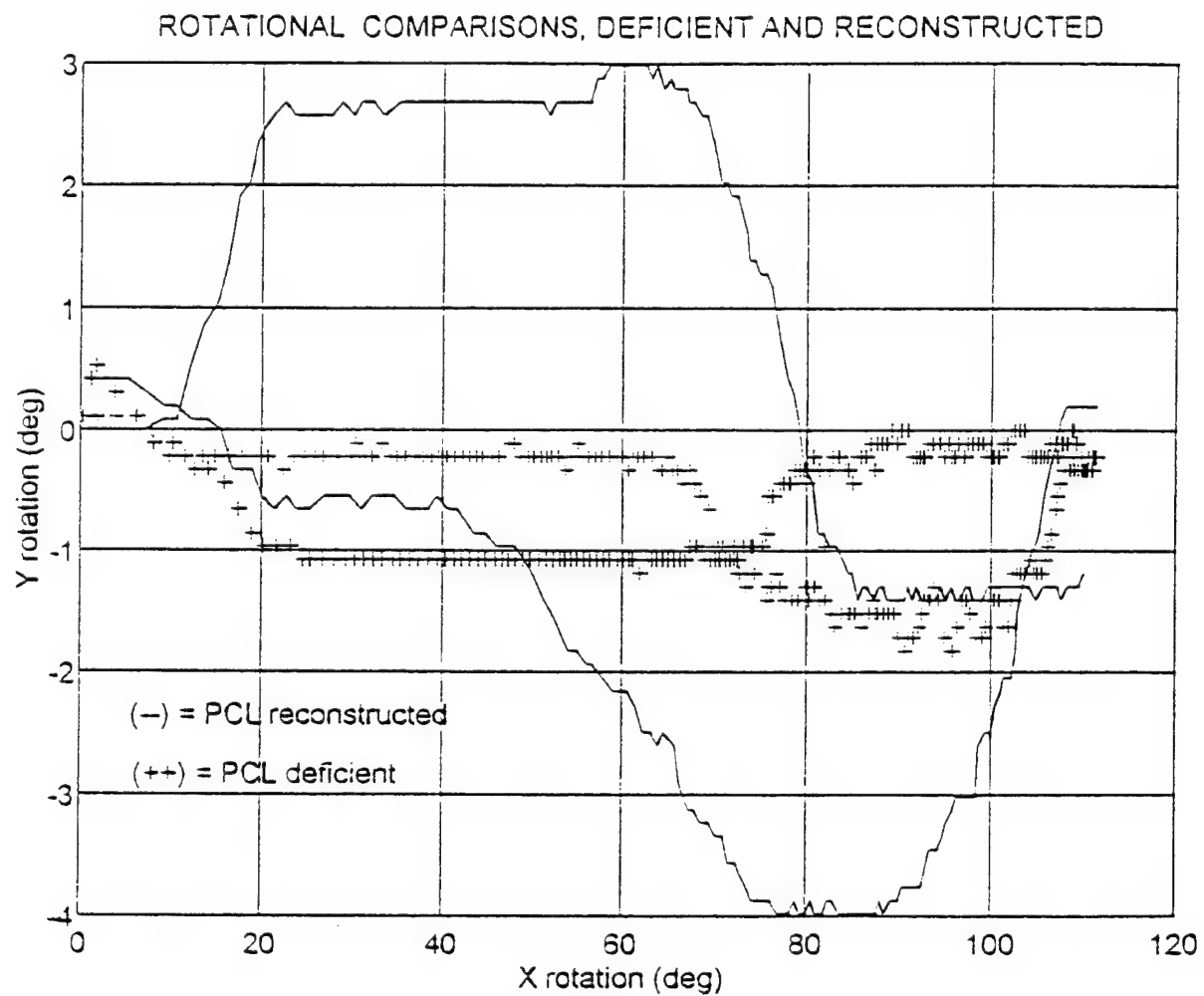


Figure 30: Y rotation of a reconstructed knee compared to a PCL deficient.

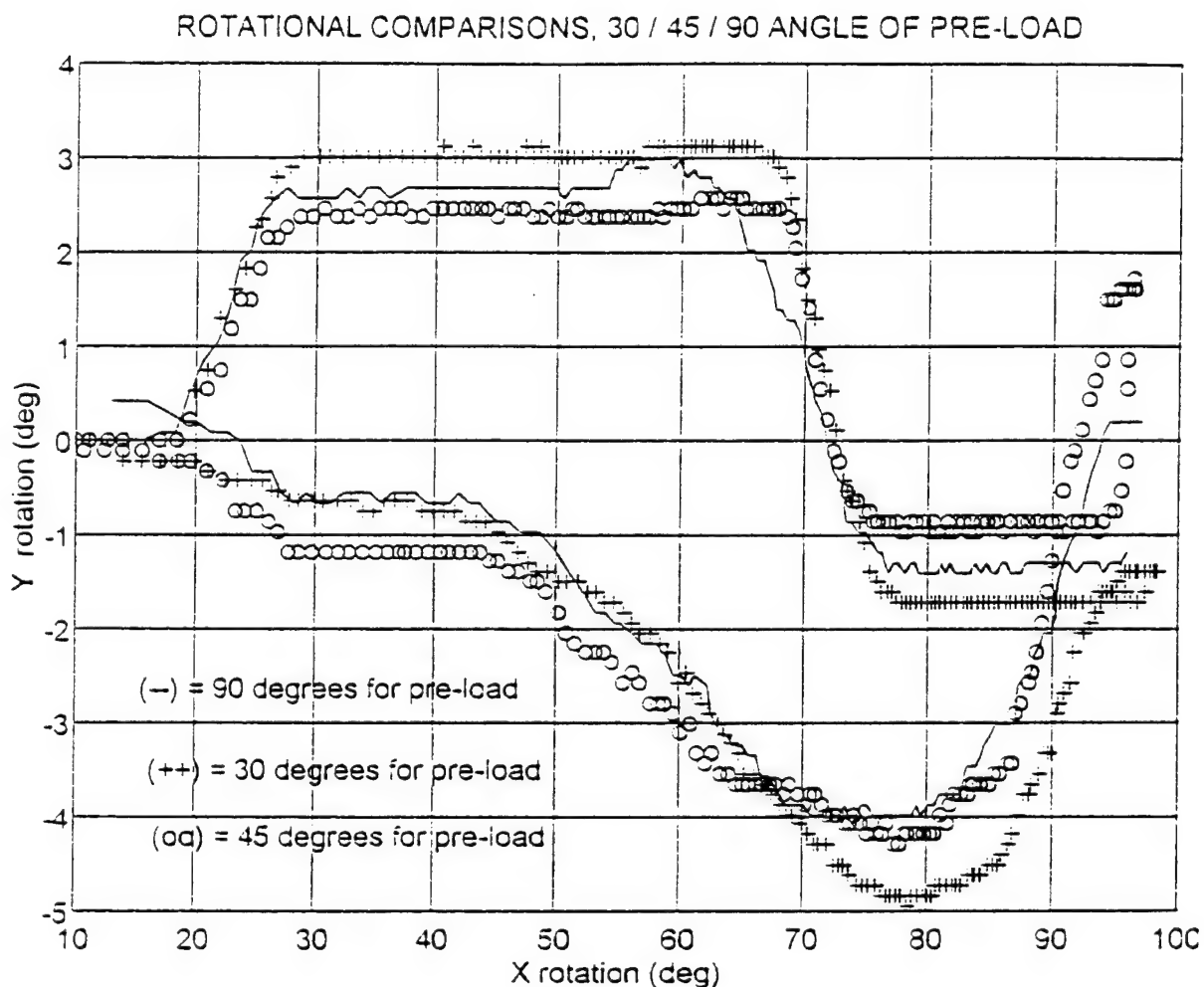


Figure 31: Reconstruction with a pre-load of 20# applied at different angles (30° , 45° , and 90°). There is little change in the curves, indicating that the angle of the pre-load is not important.

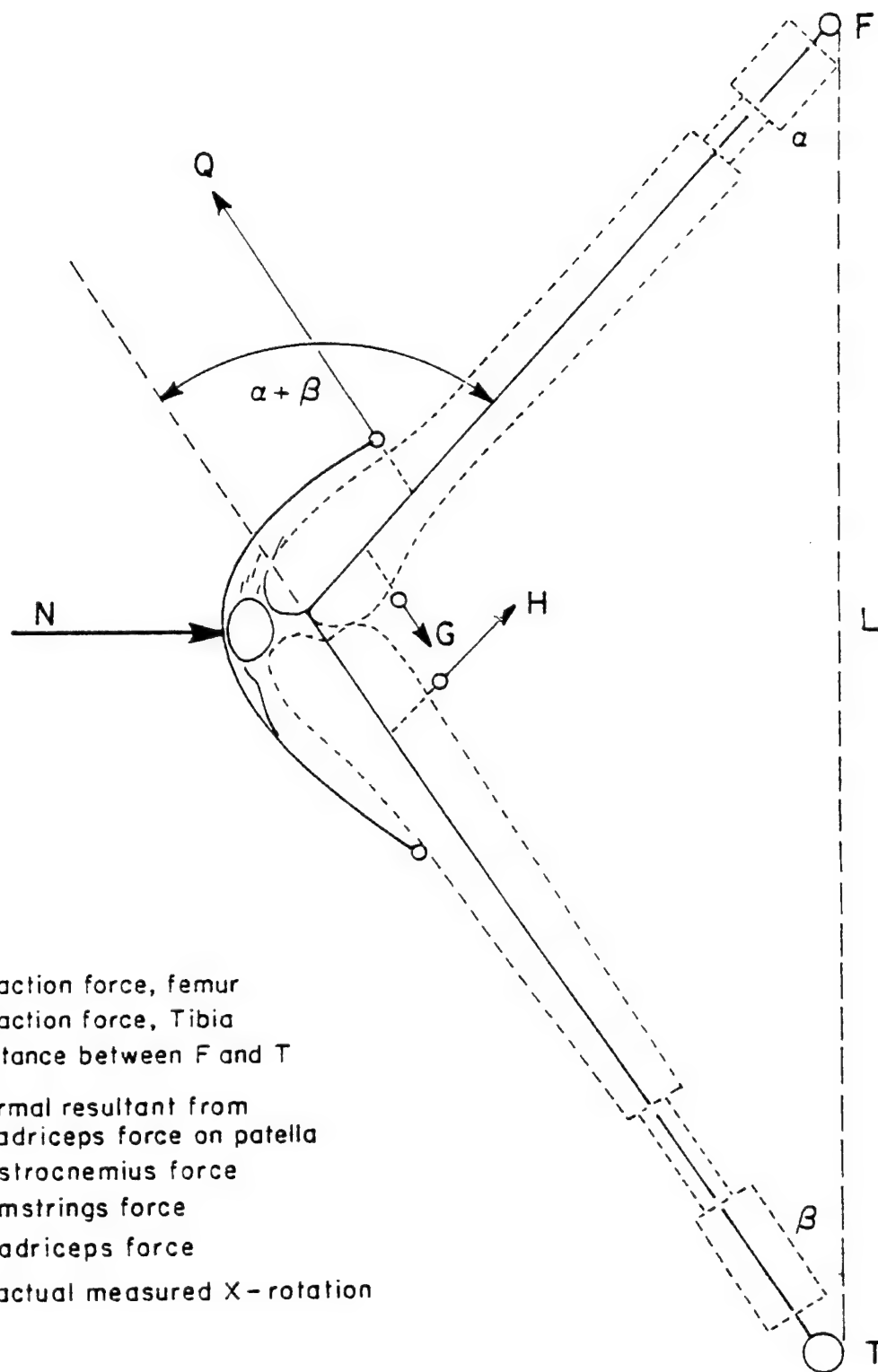


Figure 32: Schematic used in the joint reaction force resolution.

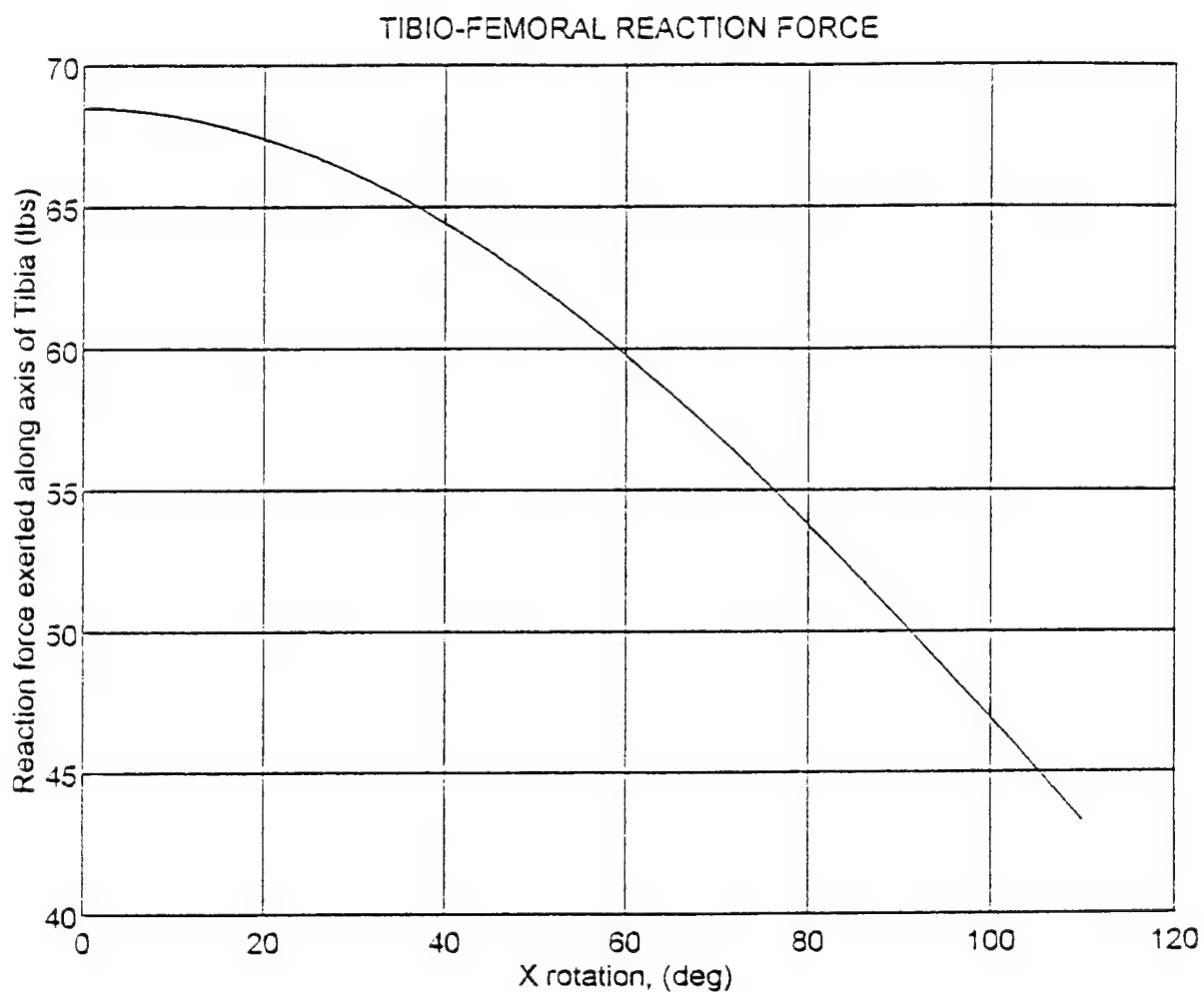


Figure 33: Sample plot of the resultant tibio-femoral reaction force.

VI. CONCLUSIONS

This six degree of freedom continuous motion and loaded model was successfully developed and applied in the study of the PCL in the human cadervic knee under several conditions. Specifically, these conditions were: PCL intact, PCL deficient, and PCL reconstructed.

Four knee specimens were used for the study. In all cases, and under all test conditions, similar results were achieved. The patterns established with the original test knee were repeated throughout the testing with the exception of actual magnitudes.

The changes noted in the Y rotation and Z translation, between the normal condition and the PCL cut condition, confirmed what was known about the role of the PCL being responsible for preventing posterior motion of the tibia. Even large quadriceps loads in the PCL deficient knee could not reproduce the intact state.

The use of a six degree of freedom model better simulates the in vivo knee and will allow more realistic tests to be performed when studying knee injuries. The use of continuous motion will lead to a better understanding of knee injuries and result in improved surgical and recovery techniques.

The fact that the reconstructed knee showed persistently altered kinematics for both rotation and translation may account for surgical failures. Interestingly, the joint reaction forces become close to the intact state after reconstruction.

The data obtained from the reconstructed knees indicate that the two bands of the PCL, the anterolateral and postero-medial, function independently and cannot be reconstructed together. Further testing needs to be done to separate the bands into two different insertion sites and determine the impact of this change throughout the range of motions studied.

VII. RECOMMENDATIONS

- CONTINUE TO IMPROVE UPON THE TEST STAND

Different technical problems for data acquisition arose with each knee. Of these, two have already been addressed. The test stand has already been modified to change the number of measurements being taken from six to twelve, and the ball and socket joints were replaced with a system to allow direct measurement of each independent motion rather than to have to back it out vectorially. The jig is in the process of being modified.

- CONSOLIDATE THE TESTS AS MUCH AS POSSIBLE

We noted that results were not perfectly reproducible when the same tests were accomplished on different days or in a different order. This occurred due to early technical problems. We will return to the original protocol to always do the tests in the same order, reduce the number of runs under a given loading condition, and preform all the testing desired on one joint on the same day to reduce the number of possible variables in the test conditions.

- DIRECT MEASUREMENT OF ACTING FORCES

To accurately calculate the joint reaction forces, specific forces involved (Patella-femoral joint, cruciate and collateral, menisci and capsule ligaments) must be computed. For this, all weights need to be considered, including the weights of the specimen and test jig. The force induced by the worm drive must also be accounted for.

- MORE RUNS OF EACH CONDITION ARE NEEDED TO ALLOW FOR STATISTICAL ANALYSIS

The primary concern of this project was to develop and perfect the previously unreported test equipment for an unconstrained, continuous motion, six degree of freedom knee model. Once the total time for each run has been reduced through improved equipment and technique, more time will be

spent on additional runs for each given condition. The reproducibility and accuracy for each test condition may then be calculated. -

- TESTING OF THE THEORY OF TWO SEPARATE INSERTION SITES FOR THE DIFFERENT BANDS OF THE PCL

If the insertion sites are separated, it should be possible to control the excess Y rotation noticed in the reconstructed graphs, as well as eliminate the cross-over noticed when compared to the PCL intact condition of the Z translation.

GLOSSARY OF TERMS

ABDUCTION - Draw away from midline

ADDUCTION - Movement of part of body towards midline

ANTERIOR CRUCIATE LIGAMENT - Crossed shaped ligament that prevents anterior motion of the tibia

ANTERIOR/POSTERIOR DRAWER - Forward/after direction along the tibial condyles

ARTHROSCOPY - Procedure wherein an orthopedist looks into a joint with specially designed, lighted, hollow instrument

CAPSULE - Covering or sheathing

COMPRESSION/DISTRACTION - Movement along the axis of the long bones of leg

CONDYLE - Rounded portion of bones, usually at joints

CRUCIATE - Crossed shaped

EPIDEMIOLOGY - Study of occurrence and prevalence of disease, often applied to study of manner of spread of disease

EXTENSION - Stretching or straightening of a limb which is contracted, dislocated, or fractured

FEMUR - Long bone in the leg; extending from hip joint to knee

FLEXION - Bending motion

GASTROSOLEUS/GASTROCNEMIUS - Main calf muscle in back of leg; action bends foot downward

HAMSTRINGS MUSCLE - Powerful thigh muscle in back of thigh, bends the knee

HYPER-EXTENDED - Extended beyond the point of equilibrium

LIGAMENT - Tough connective tissue that holds bones together

MEDULLARY - canal in the center of the leg bones

MENISCUS (pl: MENISCI) - Crescent shaped cartilage lying on tibial bone within knee joint; frequently torn in athletic injury

PATELLA - Knee-cap

PATHOKINEMATICS - Dealing with the nature of the kinematics

POSTERIOR CRUCIATE LIGAMENT - Crossed shaped ligament that

prevents tibia from moving towards the rear

QUADRICEPS FEMORIS - Large muscle in front of thigh;
straightens knee cap

SOLEUS MUSCLE - One of 2 large muscles of the calf of the leg

SCREW-HOME MECHANISM - manner in which the knee joint returns
to its normal, fully extended position

TENDON - Fibrous portion of muscle which extends to their
attachment to bones

TIBIA - Larger of 2 leg bones located on inner side of leg and
responsible for weight bearing

TIBIOFEMORAL - Pertaining to the tibia and femur

TRANSEPICONDYLAR - Across the lateral axis of the condyle

VALGUS - Turning out of the foot

VARUS - Turned in foot deformity; bowleggedness

LIST OF REFERENCES

1. Grood, E. S., Suntay, W. J., Noyes, F. R., and Butler, D. L.: Biomechanics of the Knee-Extension Exercise - Effect of cutting the Anterior Cruciate Ligament, J Bone and Joint Surg, Vol. 66-a, No. 5 pp. 725-733.
2. Noyes, F. R., Butler, D. L., Grood, E. S., Zernicke, R. F., and Hefzy, M. S.: Boimechanical Analysis of Human Ligament Grafts used in Knee-Ligament Repairs and Reconstructions, J Bone and Joint Surg, March 1984, pp. 344-352.
3. Gollehon, D. L., Torzilli, P. A., and Warren, R. F.: The Role of the Posterolateral and Cruciate Ligaments in the stability of the Human Knee, J Bone and Joint Surg, Vol. 69-A, No. 2, pp. 233-241.
4. Hollister, A. M., Jatana, S., Singh, A. K., Sullivan, W. W., and Lupichuk, A. G.: The Axes of Rotation of the Knee, Clin Orthop Rel Res, No. 290, pp. 259-268.
5. Grood, E. S., Walz-Hasselfeld, K. A., Holden, J. P., Noyes, F. R., Levy, M. S., Butler, D. L., Jackson, D. W., and Drez, D. J.: The Correlation Between Anterior-Posterior Translation and Cross-Sectional Area of Anterior Cruciate Ligament Reconstructions, J Orthop Res, Vol. 10, No. 6, pp. 878-885.
6. Fukubayashi, T., Torzilli, P. A., Sherman, M. F., and Warren, R. F.: An in vitro Biomechanical Evaluation of Anterior-Posterior Motion of the Knee, J Bone and Joint Surg, Vol. 64-A, No. 2, pp. 258-264.
7. Grood, E. S., Stowers, S. F., and Noyes, F. R.: Limits of Movement in the Human Knee - Effect of Sectioning the Posterior Cruciate Ligament and Posterolateral Structures, J Bone and Joint Surg, Vol. 70-A, No. 1 pp. 88-96.
8. Butler, D. L., Noyes, F. R., and Grood, E. S.: Ligamentous Restraints to Anterior-Posterior Drawer in the Human Knee, J Bone and Joint Surg, Vol. 62-A, No. 2, pp. 259-269.
9. Grood, E. S., Hefzy, M. S., and Lindenfield, T. N.: Factors affecting the region of most isometric femoral attachments - Part I: The posterior cruciate ligament, Am J Sports Med, Vol. 17, No. 2, pp. 197-207.
10. Hefzy, M. S., Grood, E. S., and Noyes, F. R.: Factors affecting the region of most isometric femoral attachments -

Part II: The anterior cruciate ligament, Am J Sports Med, Vol. 17, No. 2, pp. 208-216.

11. Woo, S. L-Y., Livesay, G. A., and Engle, C.: Biomechanics of the Human Anterior Cruciate Ligament - ACL Structure and Role in Knee Motion, Orthop Rev, July 1992, pp. 835-842.
12. Wascher, D. C., Markolf, K. L., Shapiro, M. S., Finerman, G. A.: Direct in Vitro Measurements of Forces in the Cruciate Ligaments - Part I: The Effect of Multiplane Loading in the Intact Knee, J Bone and Joint Surg, Vol. 75-A, No. 3, pp. 377-386.
13. Lieb, F. J. and Perry, J.: Quadriceps Function, J Bone and Joint Surg, Vol. 50-A, No. 8, pp. 1535-1547.
14. Hungerford, D. S., and Barry, M.: Biomechanics of the Patellofemoral Joint, Clin Orthop Rel Res, No. 144, Oct 1979, pp. 9-15.
15. Hollis, J. M., Takai, S., Adams, D. J., Horibe, S., and Woo, S. L.-Y.: The Effects of Knee Motion and External Loading on the Length of the Anterior Cruciate Ligament (ACL): A Kinematic Study, ASME J Biomech Eng, Vol. 113, May 1991, pp. 208-214.
16. Lewis, J. L., Lew, W. D., Hill, J. A., Hanley, P., Ohland, K., Kirstukas, S., and Hunter, R. E.: Knee Joint Motion and Ligament Forces Before and After ACL Reconstruction, ASME J Biomech Eng, Vol. 111, May 1989, pp. 97-111.
17. Dortmans, L., Jans, H., Sauren, A., and Huson, A.: Nonlinear Dynamic Behavior of the Human Knee Joint - Part I: Postmortem Frequency Domain Analysis, ASME J Biomech Eng, Vol. 113, Nov 1991, pp. 387-396.
18. Jans, H. W. J., Dortmans, L. J. M. G., Sauren, A. A. H. J., and Huson, A.: An Experimental Approach to Evaluate the Dynamic Behavior of the Human Knee, ASME J Biomech Eng, Vol. 110, Feb 1988, pp. 69-73.
19. Zavatsky, A. B., and O'Connor, J. J.: A model of human knee ligaments in the sagittal plane - Part 1: response to passive flexion, J Eng in Med, Vol. 206, pp. 125-134.
20. Zavatsky, A. B., and O'Connor, J. J.: A model of human ligaments in the sagittal plane - Part 2: fiber recruitment under load, J Eng in Med, Vol. 206, pp. 135-145.

21. Blankevoort, L., Huiskes, R., de Lange, A.: Recruitment of Knee Joint Ligaments, ASME J Biomech Eng, Vol. 113, Feb 1991, pp. 94-103.
22. Goodfellow, J., Hungerford, D. S., and Zindel, M.: Patello-femoral Joint Mechanics and Pathology - 1. Functional Anatomy of the Patello-femoral joint, J Bone and Joint Surg, Vol. 58-B, No. 3, pp. 287-290.
23. Grood, E. S., Stowers, S., and Noyer, F. R.: Flexibility Studies of the Human Knee: An approach to Differential Diagnosis of Ligament Injuries.
24. Garg, A., and Walker, P. S.: Prediction of Total Knee Motion using a Three Dimensional Computer model, J Biomech, Vol. 23, No. 1, pp. 45-58.
25. Huber, H., and Mattheck, C.: The cruciate ligaments and their effect on the kinematics of the human knee, Med and Biol Eng and Comput, No. 26, pp. 647-654.
26. Wongchaisuwat, C., Hemami, H., and Hines, M.: Control exerted by Ligaments, J Biomech, Vol. 17, No. 7, pp. 525-532.
27. Bishop, R. E. D.: On the mechanics of the human knee, J Eng in Med, Vol. 6, No. 2, pp. 46-52.
28. Butler, D. L., Sheh, M. Y., Stouffer, D. C., Samaranayake, V. A., and Levy, M. S.: Surface Strain Variation in Human Patellar Tendon and Knee Cruciate Ligaments, ASME J Biomech Eng, Vol. 112, Feb 1990, pp. 38-45.
29. Pennock, G. R., and Clark, K. J.: An anatomy based coordinate system for the description of the kinematic displacements in the human knee, J Biomech, Vol. 23, No. 12, pp. 1209-1218.
30. Reilly, D. T., and Martens, M.: Experimental Analysis of the Quadriceps muscle force and patello-femoral joint reaction force for various activities, Acta orthop Scandinavia, No. 43, pp. 126-137.
31. Basic Biomechanics of the Musculoskeletal System: Biomechanics of Knee Joint, Margareta Nordin, Victor H. Fromkel; 1980 2nd Edition Lea and Febiger Publishers.
32. Knee Ligaments: Structure, Function, Injury and Repair; Editors: Dale Daniel, Wayne Akeson, John O'Connor; Raven press 1990.

INITIAL DISTRIBUTION LIST

	No. Copies
1. Defense Technical Information Center Cameron Station Alexandria, Virginia 22304-6145	2
2. Library, Code 52 Naval Postgraduate School Monterey, California 93943-5101	2
3. Chairman, Code ME/Kk Department of Mechanical Engineering Naval Postgraduate School Monterey, California 93943-5000	1
4. Professor Young W. Kwon, ME/Kw Department of Mechanical Engineering Naval Postgraduate School Monterey, California 93943-5000	2
5. Naval/Mechanical Engineering, Code 34 Naval Postgraduate School Monterey, California 93943-5000	1
6. David Adkison, M.D. CDR, Medical Corps Department of Orthopaedic Surgery Naval Hospital Oakland, California 94627	3
7. Marlene De Maio, M.D. LCDR, Medical Corps Department of Orthopaedic Surgery Naval Hospital Oakland, California	3
8. James T. Scholfield, ME/Sc Department of Mechanical Engineering Naval Postgraduate School Monterey, California 93943-5000	1
9. LCDR Robin L. Belen 232 West 234th Place Carson, California 90745	1